DETECTION AND ESTIMATION OF DAMAGE IN FRAMED STRUCTURES USING EXPERIMENTAL MODAL DATA

W. A. R. K. De Silva

188036D

Degree of Master of Science

Department of Civil Engineering

University of Moratuwa

Sri Lanka

January 2020

DETECTION AND ESTIMATION OF DAMAGE IN FRAMED STRUCTURES USING EXPERIMENTAL MODAL DATA

W. A. R. K. De Silva

188036D

Thesis submitted in partial fulfilment of the requirements for the degree Master of Science in Civil Engineering

Department of Civil Engineering

University of Moratuwa

Sri Lanka

January 2020

DECLARATION

I declare that this is my own work and this thesis does not incorporate without acknowledgement any material previously submitted for a Degree or Diploma in any other University or institute of higher learning and to the best of my knowledge and belief it does not contain any material previously published or written by another person except where the acknowledgement is made in the text.

Also, I hereby grant to University of Moratuwa the non-exclusive right to reproduce and distribute my thesis, in whole or in part in print, electronic or other medium. I retain the right to use this content in whole or part in future works (such as articles or books)

………………………………………   Date:

W. A. R. K. De Silva

The above candidate has carried out research for the Masters under my supervision.

………………………………………   Date:

 Dr. C. S. Lewangamage

………………………………………   Date:

 Prof. M. T. R. Jayasinghe

ABSTRACT

The inevitable ageing and degradation of buildings and the structural failures that follow, have ignited a need for early prognosis of probable structural failures so that proactive measures can be undertaken. Hence, one of the important steps of structural health monitoring (SHM) process is the detection of damage and estimation of damage severity. Modal data can be effectively used for this purpose owing to their sole dependency on mechanical characteristics of a structure. However, the focus of mode shape-based damage detection techniques has concentrated only on symmetric structures whereas the existing buildings are typically asymmetric. This study presents a damage detection methodology using the behaviour of mode shape derivatives such as mode shape slope and mode shape curvature for a symmetric framed structure applied on an experimental model tested using a shaking table, and a calibrated finite element model. Furthermore, an extended parametric analysis has been performed to investigate damage localization and quantify severity. Finally, the models have been modified to incorporate the irregularity effects and damage detection possibility has been explored. The study enables to provide key conclusions for damage detection with respect to localization and severity in the steel frame model. Damage detection method using the mode shape curvature is identified to be more sensitive as opposed to mode shape slope method. And the effect of mass irregularity on the detection methods were identified.

Key words: structural health monitoring, modal based damage detection, damage localization, damage severity, frame structure, shaking table, finite element model, irregularity

DEDICATION

To my loving parents and sisters for encouraging me throughout the milestones of my life and my supervisor, Dr. C. S. Lewangamage and co-supervisor Prof. M.T.R. Jayasinghe for the unwavering motivation and mentorship they provided.

ACKNOWLEDGEMENT

CONTENTS

LIST OF FIGURES

LIST OF TABLES

LIST OF ABBREVIATIONS

Abbreviation	Description
SHM	Structural Health Monitoring
NDT	Non-destructive testing
VBDD	Vibration based detection
MSS	Mode shape slope
MSC	Mode shape curvature
DOF	Degrees of freedom
DMSS	Difference of mode shape slope
DMSC	Difference of mode shape curvature
CDM	Central difference method

CHAPTER I

1. BACKGROUND

1.1. Introduction

Research on Structural Health Monitoring (SHM) initiated from 1980's and if one performs a document search on the research database 'Scopus' for this phrase, approximately 24,000 results can be obtained, last decade undoubtedly contributing the highest number of related studies. From the earliest monitoring methods such as tap-testing to modern real time wireless sensor networks, SHM arena has demonstrated a conspicuous multidisciplinary advancement. However, the industrial deployment of such strategies is still at a slow pace.

Historically, dams are the first class of structures that were mandated for regular inspection following the Dale Dyke Dam failure in Sheffield (1864), United Kingdom, which was a devastating event taking 254 human lives (Figure 1-1). In 1937 the earliest systematic documentation of bridge monitoring was reported by Carder (1937) on the Golden Gate and Bay Bridges in San Francisco. The study focused on measuring periods of structural components during construction to understand the dynamic response and consequences of possible earthquakes (Figure 1-2).

Figure 1-1- Dale Dike Dam failure (Brownjohn, 2007)

Figure 1-2- San Franssco and Bay Bridge (Cardr 1937)

The need for monitoring structural safety is presumably at a growing rate due to the ever increasing complexity of structures and structures with exceeded life spans which has resulted in increased susceptibility to failures. SHM is related with 4 levels of damage identification states (Chen & Ni, 2018) (Doebling, Farrar, & Prime, 1998), namely, damage detection, localization, severity and prognosis. From the numerous damage identification methods vibration based methods are capable of achieving higher levels of the above states because of the global nature of the method. This method is based on identifying the changes of modal properties due to deviations in physical properties induced from damages. Mode shape, Natural frequency or modal damping characteristics can be used as damage indicators. The initial studies have explored in to modal frequency and mode shape methods and with the development of research base the limitations of such methods have been established, which would be discussed in length in the literature review (Chapter 2) of the thesis.

On comparison of the mode shape of damaged and undamaged structures, a damage indicator can be established (Kaloop & Hu, 2016), but this method has limitations such as the need of a dense array of sensors and noise contamination issues (Fan & Qiao, 2011). Therefore, it has been concluded that the detectability of mode shape is less sensitive for damage and that investigation should be shifted to mode shape derivatives.

Mode shape slope (MSS) and mode shape curvature (MSC) are the first and second derivatives of the mode shape. The initial damage related study on MSC was conducted on cantilever and simply supported analytical beam models (Pandey et al., 1991).
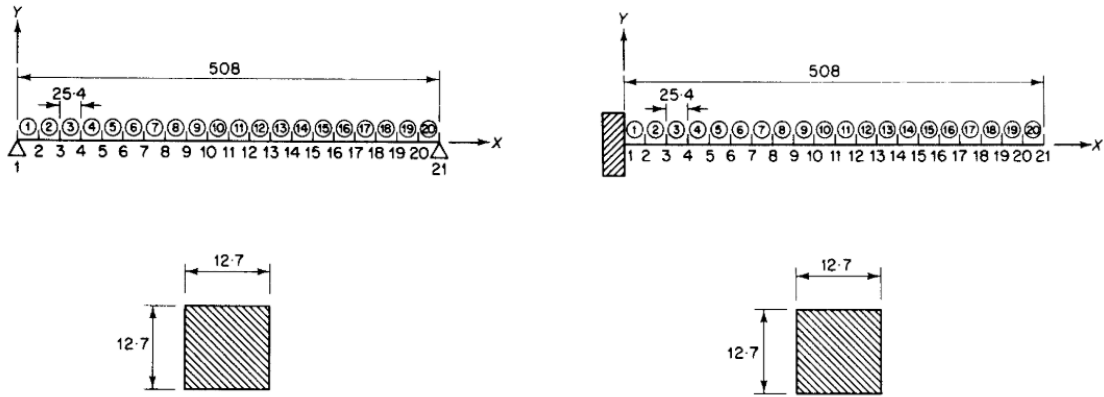
Figure 1-3- Cantilever and simply supported analytical beam models used by Pandey et al. (1991)

Following this study, the MSC methods have been applied for damage detection and localization in numerical and experimental beam models (discussed in Chapter 2). However, this method has not been implemented on real scale structures nor on frame models to explore the 3rd level of SHM objectives, namely, damage quantification. Moreover, the accuracy of this method on regular and irregular framed structures is yet to be elucidated.

1.2.   Importance and Identification of Knowledge Gap

Modal data based structural damage identification techniques have been established as a popular method, due to the ease of physical interpretation of modal parameters with the behaviour of structures.

It should be noted that the objectives of SHM (as described in Section 1.1) pave the pathway for achieving an optimum damage identification so that structural safety can be ensured. However, by reviewing the modal data-based studies it is evident that only the first two levels (damage detection and localization) have been

assessed in a comprehensive manner with an insufficient focus on the third level (damage quantification).

Moreover, on comparison of the research conducted thus far, it is apparent that the mode shape derivatives are sufficiently sensitive to damages. However, the use of MSS and MSC have majorly been limited to simple structural elements, whereas the exploration with respect to frame structures have limited number of research conducted.

With the advancements of structural engineering discipline, the uniqueness and complexity of buildings have increased, where structural irregularities come in to play. Therefore, it is important to explore the possibilities of applying the above said MSS or MSC methods for detection of damages in irregular structures.

Henceforth, the need of investigating the applicability of damage detection, localization and quantification methods using mode shape derivatives (MSS and MSC) on regular framed structures and exploring the implications on irregularity has been identified. Hence, the objective of this research is to bridge the knowledge gap concerning damage identification for frame structures.

1.3.   Objectives of the Research

This research utilizes a modal-based structural damage identification technique for a framed structure to obtain the following objectives,

I.   Damage detection capability for an experimental shaking table model of a regular frame structure

II.   Damage localization and severity capabilities by performing a parametric analysis on a validated finite element (FE) model

III.   Effect of irregularity on the results of the technique

1.4.   Methodology

The scope of the study was limited to determining the damage detection, localization and severity potential of mode shape derivatives (MSS and MSC) for a regular frame structure using an experimental and a finite element model. Furthermore, the effect of

irregularity on the above said damage indicators was investigated by extending the analysis to an irregular frame structure.

The methodology describes the utilized numerical formulation, experimental model and the finite element model for the regular frame structure, followed by the extended analysis for an irregular framed structure.

1.5. Arrangement of the Report

Chapter 1 presents the background of the study. An introduction to the modal based damage detection techniques, discussion on the knowledge gap, objectives of the study and the summary of the methodology are described.

Chapter 2 describes a review of previous work found in literature by giving an introduction to structural health monitoring (SHM), structural damage and damage identification based on modal properties.

Chapter 3 Initially the numerical technique on using properties of mode shape slope and mode shape curvature distributions are described.

Chapter 4 contains the work carried out with the experimental framed model. The fabrication of preliminary and improved experimental shaking table model, testing procedure for both the regular and irregular models are discussed in length.

Chapter 5 presents the finite element model development and the parametric study for damage localization and damage severity. Also the work done for irregular model focusing on the mass-irregularity is described.

Chapter 6 provides a discussion on the results for mode shape derivatives based damage detection and damage severity using the experimental and finite element studies. Moreover, the results of the irregular experimental and finite element models are also discussed.

Chapter 7 discusses the conclusions of the work, the feasibility of this method to implement for real scale structures and the future work required for a further understanding of the method.

CHAPTER II

2. REVIEW OF PREVIOUS LITERATURE

2.1. Structural Health Monitoring

The world is witnessing an exponential growth in advancements related to infrastructure development producing taller and complex structures day by day, which in turn has increased the susceptibility to failure and the requirements of structural health monitoring (SHM). The earliest monitoring of structures has presumably initiated from large construction projects such as dams, off-shore installations and long-span cable-supported bridges (Brownjohn, 2006). Gradually the need of observing and evaluating the loading and response behaviour of buildings and towers (Farrar & Worden, 2007) has led to the development of automated SHM systems (Chen & Ni, 2018).

Using an automated monitoring system to observe and assess operational health of a structure is the basis of SHM. The system strategy consists of sensor networks, data processing and sensor fusion algorithms, an analysis engine for combining modal identification techniques and numerical results and damage diagnosis and prognosis systems (Figure 2-1).

SHM is a global vibration-based system in contrast with the non-destructive testing methods that are commonly used in local damage assessment in structures. Visual inspection, ultrasound, acoustic emissions, thermography and electromagnetic methods are some of the non-destructive testing examples. Nevertheless, with the recent development of SHM systems the response of the structure can be examined with real-time measurements. However, owing to the multi-disciplinary nature, advanced technology needed, and the large data flows incorporated, the industrial deployment of such systems is still at an infancy stage (Peter Cawley, 2018).
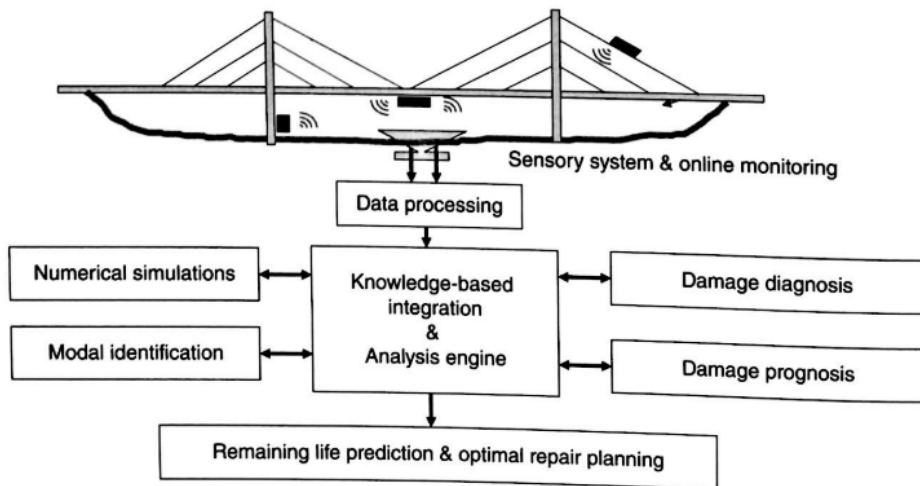
Figure 2-1- Integrated framework for structural health monitoring (Chen & Ni, 2018)

2.2.   Structural Damage Identification

Structural damage is defined as alterations in geometric or material properties inclusive of deviations in connectivity and boundary conditions that adversely affect the performance of a structure (Farrar & Worden, 2007). The scale, severity and accumulation of damage depend on the environmental and loading conditions, life-span of the structure as well as the localization of the anomalies. Therefore, early identification is paramount for the prevention of progression of damage, probable structural catastrophes and loss of human life. The main motivations of SHM is based on damage identification and the objectives are classified as follows (Chen & Ni, 2018) (Doebling et al., 1998);

- Level I: Damage detection
- Level II: Damage localization
- Level III: Damage severity
- Level IV: Damage prognosis

Methods utilized in damage identification can be mainly categorized under non-destructive testing (NDT) and vibration-based detection (VBDD), from which higher levels of the above objectives can be achieved by the latter method owing to

the global nature of output (Chen & Ni, 2018). The vibration-based methods are derived using the functional relationships between vibrational characteristics (mode shape, Eigen frequency, modal damping etc.) and physical properties (stiffness, mass, damping) of a structure (Fan & Qiao, 2011) where damage induced deviations in physical properties provide quantitative indications through changes in modal behaviour (Rytter, 1993) . The possibility of clearly visualizing and interpreting these modal properties with physical meanings, as opposed to mathematical formulations, has resulted in gaining recognition of this method among researchers. Following section presents the key vibration features that has been explored in literature focusing mainly on the mode shape derivatives.

2.3. Damage Detection and Localization Based on Changes in Modal Properties

The gradual progression of damage detection using vibrational features can be identified by chronologically listing the related literature, where modal frequency, mode shape and mode shape derivatives (mode shape slope (MSS), mode shape curvatures (MSC)) have been explored.

The initial studies were focused on developing relationships between natural frequency variations and damages using various experimental and numerical methods (P Cawley & Adams, 1979). However, modal frequency shows less sensitivity in localized damage detection due to the effects from boundary conditions, environmental conditions and mass variations (Peter Cawley, 2018) (Fan & Qiao, 2011) and fails to provide spatial information about damage (Doebling et al., 1998). In comparison, mode shapes and mode shape derivatives are capable of addressing the limitations related to modal frequency based methods owing to the spatial information included and the less effect from environmental conditions (Fan & Qiao, 2011).

The fundamental approach behind the mode shape-based damage detection is the comparison of modal data of undamaged and damaged structures. Research thus far has investigated the applicability of these damage indicators, using traditional mode shape based methods and modern signal-processing methods (Kaloop & Hu, 2016), while emphasizing on the inherent limitations such as the requirement of a dense series

of sensors and the probable noise contamination issues (Fan & Qiao, 2011). Consequently, it has been found that the fundamental mode shape is less sensitive for damage localization even with a high number of sensors (Roy, 2017).

Therefore, the focus has shifted to using derivatives of mode shapes as an effort to enhance the sensitivity. The first and second derivatives of mode shape, namely, MSS (Zhu, Li, & He, 2011) and MSC (Pandey, Biswas, & Samman, 1991)(Altunışık, Okur, Karaca, & Kahya, 2019)(Wahab & Roeck, 1999)(Dessi & Camerlengo, 2015) have been utilized for damage detection and damage localization. The initial study about MSC (Pandey et al., 1991) uses cantilever and simply supported analytical beam models to conclude that the changes in MSC between intact and damaged models reaches an absolute maximum at the location of damage and that the magnitude of the difference increase with the increase of the damage. A central difference approximation was used to obtain the MSC from the displacement mode shapes. Subsequently, the MSC method has been applied for damage detection and localization in real bridges (Wahab & Roeck, 1999) and, numerical and experimental beam models (Dessi & Camerlengo, 2015) (Altunışık et al., 2019). Furthermore, the focus has shifted to novel techniques based on mode shape analysis including modal flexibility methods (Altunışık et al., 2019) and wavelet energy methods (Ostachowicz, Radzienski, Cao, & Xu, 2018).

However, the exploration of MSS and MSC based damage identification methods, applied on framed structures are limited and the existing literature only addresses the first two levels of SHM objectives, namely, damage detection and damage localization (Zhu et al., 2011)(Roy & Ray-chaudhuri, 2013)(Roy, 2017).

2.4.   Experimental models used in related literature

Beskhyroun, Oshima, Mikami, & Tsubota (2006) used changes in   Power Spectral Density (PSD) for damage identification and the developed algorithm is applied to experimental steel bridge model and a book-shelf model. The experiments with the 3-storey steel frame book-shelf structure is noted for this study. The structure is fabricated using uni-strut columns, Aluminium plates and support brackets and it is mounted on 4 air mount isolators (Figure 2-2). An external shaker is used to provide

random vibration inputs. The release of bolts between plates and columns, removal of brackets and reducing torque of bolts are the cases that was used for introducing damage to the structure. This method of damage inducement has been studied for the preliminary model in this thesis. However, the algorithm does not provide sufficient output to quantify the damage scenarios.
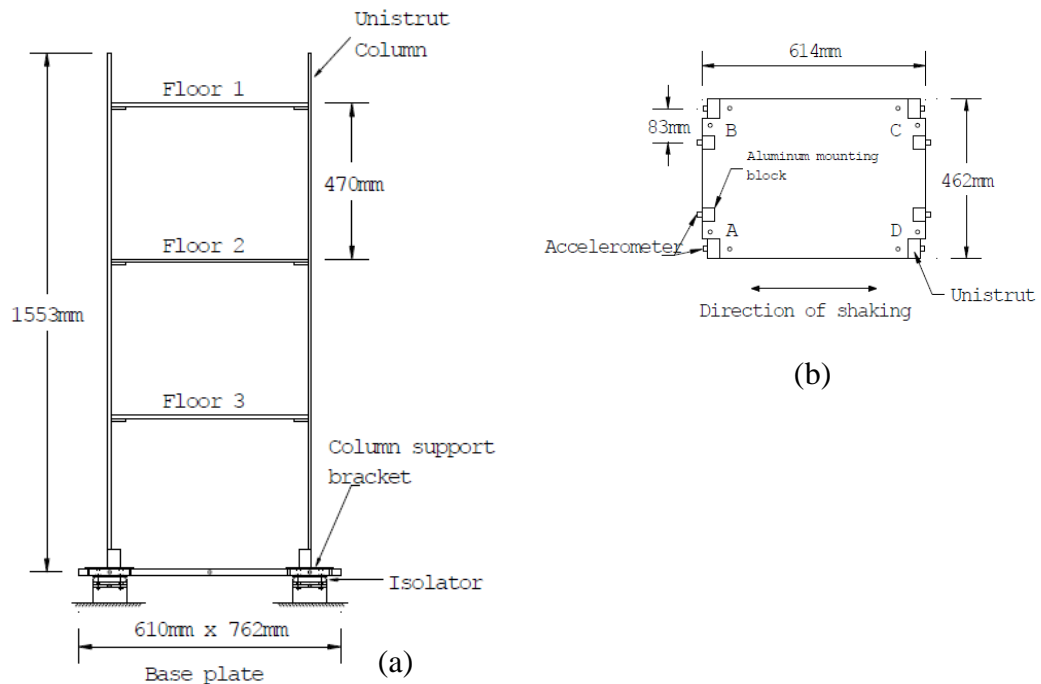
Figure 2-2. Basic dimensions of the 3-storey frame structure (a) side elevation and (b) floor layout (plan elevation) (Beskhyuroun et al. 2006)

Mode shape, damping ratio and modal frequency changes during induced damage when the peak ground acceleration (PGA) is increased until failure are observed in Gong, Xie, & Ou (2008). Shaking table tests were conducted on a 12-storey reinforced concrete frame with a base size of 0.6 m x 0.6 m (refer Figure 2-3). Strong ground motions such as EL Centro wave, Kobe wave and Shanghai artificial wave were applied on the structure. It was observed that the modal frequency decreases and damping ratios increase with the accumulation of damage when the earthquake input is increased. Even though, the study does not focus on damage identification techniques, the fabrication of structure model deemed beneficial.
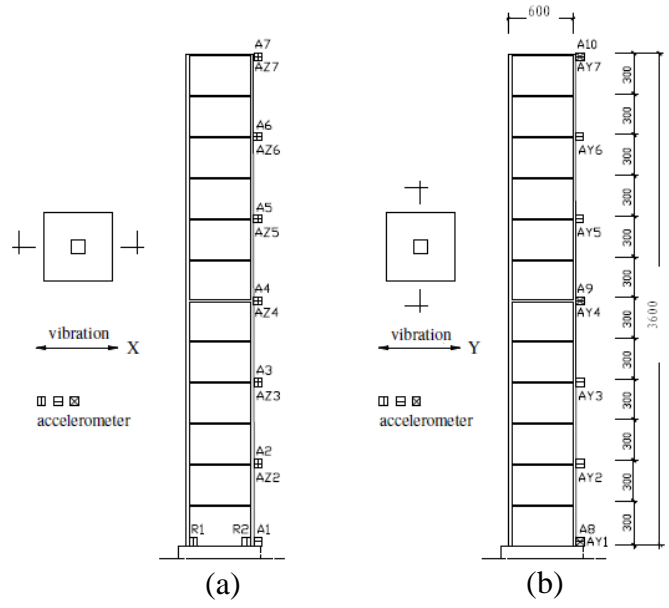
Figure 2-3 Accelerometer locations and orientations of the R/C frame model (a) X-plane (b) Y-plane (Gong et al. 2008) (legend shows the 3-axis accelerometers)

Zhu et al. (2011) used changes in first mode shape slopes for single and multiple damage detection scenarios and the method was applied on a 3-storey steel frame model and subjected to a white noise random ground excitation using a shaking table (refer Figure 2-4).
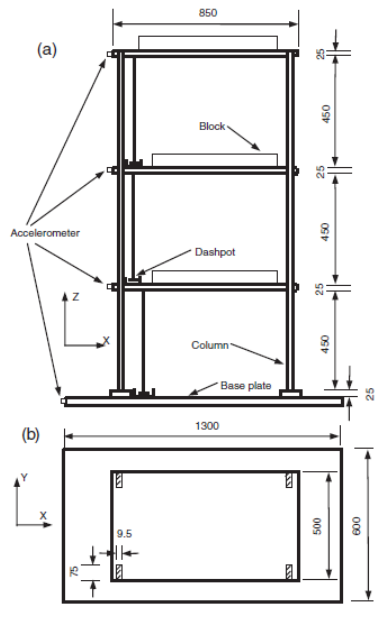
Figure 2-4 A three-storey steel model used in Zhu et al. (2011) for experimental shaking table tests (a) side elevation (b) plan elevation. (all dimensions in mm)

Furthermore, experimental shaking table tests conducted in Kim, Lee, & Ngo-Huu, (2007) and Wu, Yamazaki, Sawada, Sakata, & Asce (2018) were studied for understanding optimum placement of accelerometers, techniques in fabrication and other factors related to shaking table tests.

Mounting of accelerometers on the experimental model needs to be carefully considered to prevent the adverse effects such as influencing the structural response (due to stiffness changes from a using a heavy sensor) and recording the incorrect translational directions. Therefore, when designing the experimental model, the weight of each frame need to be significantly higher than the accelerometer and cable weight, so that the effects would be minor. Furthermore, the fixing the sensors as a stud mount (Figure 2-5) is recognized as the optimum method (Gürkan, Gürkan, & Dindar, 2018) (Kim, Lee, & Ngo-Huu, 2007) (Wu, Yamazaki, Sawada, Sakata, & Asce 2018).
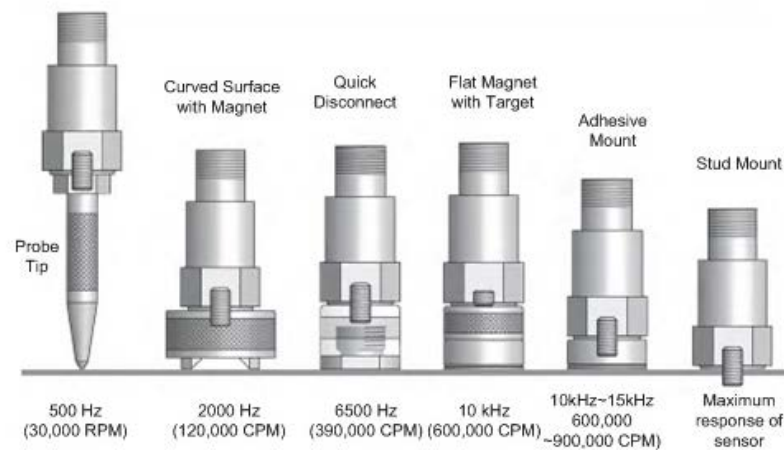
Figure 2-5 Methods of mounting for sensors

CHAPTER III

3. NUMERICAL FORMULATION

3.1.   Fundamentals of mode shape derivatives for damage identification

As highlighted in the "Introduction" the usage of modal properties for the damage assessment process has evolved exponentially from using resonance frequency to using derivatives of mode shapes. But for the latter case, most of the applications have been limited to beams and plates. Since, most structural components can be simplified as beams or plates, these research create a benchmark for accuracy and the effectiveness of the damage identification techniques.

Curvature of a beam is related to the flexural stiffness of a beam cross-section, which can be defined as follows:

$$\emptyset^{ll} = M/EI \qquad (1)$$

Here, for a cross-section, $\emptyset^{ll}$ is the curvature, M the bending moment, E is the modulus of elasticity and I is the second moment of area. For a certain localized damage, the stiffness (EI) of that section would decrease. Accordingly, the magnitude of the curvature would be increased. This provides the fundamental theory behind a damage detection scheme using MSC, where the differences between the MSC of an undamaged and damaged structure can be observed to derive conclusions (Pandey et al., 1991).

3.2.   Mode shape slope and mode shape curvature

As a step forward from simple elements, this study captures the applicability of the above method for frame structures. For a spring mass system with n degrees-of-freedom (DOF) numerical formulations for difference of MSS (DMSS) and difference of MSC (DMSC) have been derived (Roy, 2017). For large values of n (n $\rightarrow \infty$), the DMSS reaches $+\infty$ at the damage location and the DMSC just before damage location and just after the damage location, reaches $-\infty$ and $+\infty$. Therefore, for a finite DOF system, at the damage location, a maximum value for DMSS and a zero crossing for DMSC can be expected.

A regular frame structure can be idealized as a vertical cantilever with fixed and free boundary conditions at the base and at the top end. Considering a uniform discretization with h being the distance between any two consecutive points, a central difference method (CDM) can be used to calculate the slope and the curvature from the mode shape (Pandey et al., 1991)(Wahab & Roeck, 1999).

$$\emptyset^l(x) = \frac{\emptyset(x+h) - \emptyset(x-h)}{2h} \tag{2}$$

$$\emptyset^{ll}(x) = \frac{\emptyset(x+h) - 2\emptyset(x) + \emptyset(x-h)}{h^2} \tag{3}$$

Here, $\emptyset(x)$ is the mode shape function and the first and second derivatives obtained in (2) and (3) give the functions of MSS and the MSC respectively. Notably, the calculation for a point x requires the mode shape values of one forward and one backward point (i.e. $\emptyset(x - h)$ and $\emptyset(x + h)$). However, for the fixed and the free boundaries, both these requirements will not be met. Therefore, the derivations are modified such that, at a fixed end the forward difference method and at a free end, the backward difference method can be used (Roy, 2017).

$$\emptyset^l(x)|\text{forward} = \frac{\emptyset(x+h) - \emptyset(h)}{h} \tag{4}$$

$$\emptyset^{ll}(x)|\text{forward} = \frac{\emptyset(x+2h) - 2\emptyset(x+h) + \emptyset(x)}{h^2} \tag{5}$$

$$\emptyset^l(x)|\text{backward} = \frac{\emptyset(x) - \emptyset(x-h)}{h} \tag{6}$$

$$\emptyset^{ll}(x)|\text{backward} = \frac{\emptyset(x) - 2\emptyset(x-h) + \emptyset(x-2h)}{h^2} \tag{7}$$

On consideration of these modifications it is evident that the effect of boundary conditions on the damage assessment accuracy need to be addressed. Furthermore, it was found that the higher modes tend to estimate multiple peak locations for DMSC, for a simple beam element (Pandey et al., 1991). Therefore, this study focuses only on the first mode shape for damage assessment.

CHAPTER IV

4. EXPERIMENTAL MODEL

4.1. Introduction

The numerical formulation for damage assessment was first applied on a frame model tested on a 1-DOF shaking table and the damage detection capability was investigated. This chapter elaborates the development and testing of the shaking table experimental model.

4.2. Shaking Table and Instrumentation

The experimental tests were conducted using uni-directional shaking table (Figure 4-1) with a deck of 500 x 700 mm and a maximum load capacity of 80 kg, at the Department of Civil Engineering, University of Moratuwa. The operational limits are, frequency range of 0-20 Hz, peak displacement of 120 mm and a peak velocity of 50 cm/s. 4 numbers of analogue accelerometers are available with a sensitivity of 1 V/g and a sampling rate of 0.001 s. A preliminary frame model was initially tested. Subsequently, a modified version was fabricated to address the limitations identified by the prior model.

Figure 4-1 Shaking table (ANCO R-201) in Department of Civil Engineering, University of Moratuwa

4.3.   Preliminary Shaking Table Modal and Learning Outcomes

A 6-storey steel frame with timber plates (geometric scale 1:20) with uniform section sizes were used as the preliminary model (Figure 4-2) to identify the characteristics and capacity of the shaking table and the measurements. For the 4 columns and 6 slabs, 6.6 mm diameter steel threaded bars and square timber plates (200 mm x 200 mm) with a thickness of 3 mm were used respectively. The steel base plate was fixed to the shaking table top using steel nuts, bolts, flat washers and spring washers for enhanced fixity. And the connection at each slab column joint consisted of the same connection details. The floor to floor height was maintained at 150 mm. Damage was induced by the loosening of bolts in different magnitudes (1 bolt/ 2 bolts/ 4 bolts per level) and in different levels.

(a)   (b)   (c)
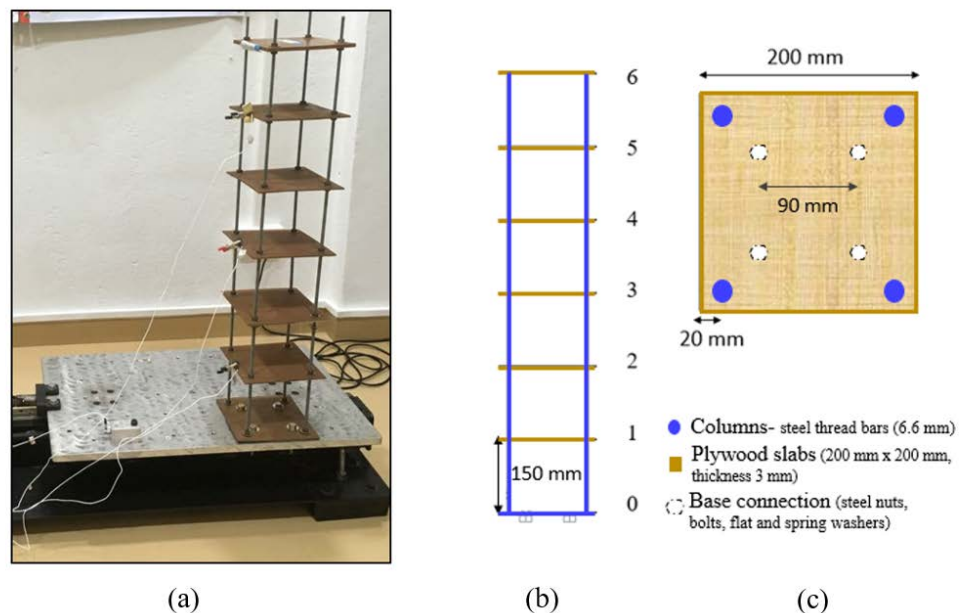
Figure 4-2- Preliminary shaking table framed model (a) mounted on shaking table deck (b) schematic diagram (side elevation) (c) plan elevation of the base slab with connections

The damage assessment was done by comparing undamaged and damaged responses. However, limitations were encountered and several learning outcomes were derived.

- The mode shape smoothness can be improved by overlapping the limited number of sensors and running several tests within one test series.

- Steps should be taken to increase the rigidity of the connections to reduce the accumulation of damage due to the input excitations.
- In order to accurately simulate the damage scenarios a method other than loosening the bolts should be investigated.
- To investigate the effects of irregularity, the model should be modified.

4.4.   Improved Experimental Modal

The design of the improved model and the instrumentation were based on the learning outcomes obtained from the preliminary model and the shaking table models in literature (Zhu et al., 2011)(Kim et al., 2007)(Ye & Jiang, 2018). Figure 4-3 shows the improved experimental model used in the study. The 7-storey steel frame model with a geometric scale of 1:20 and a floor to floor height of 180 mm, consists of steel beams and columns. Each level has monolithically connected beams with 30 mm width and 6.35 mm depth, fabricated from a steel plate (Figure 4-4). The beam-column connection consists of 4 bolts (6 mm), 8 nuts and 8 spring washers to ensure rigid connections (see Figure 4-5, Figure 4-6). Also, the steel base plate is fixed to the shaking table deck with rigid connections (Figure 4-8). These measures ensure low levels of damage accumulation and reduce the probable nonlinearities of the structure (Wahab & Roeck, 1999).

The model is fabricated in such a way that the columns and the beam sections can be dismantled at any time, section size of the columns can be varied at any level and the number of stories can be varied between 1 to 7 as required, all the while maintaining the rigidity of the connections. The typical circular steel columns are 16 mm in diameter (undamaged structure) and to induce damages, three sets of low diameter columns (12 mm, 10 mm and 6 mm) were fabricated (4 columns each) (Figure 4-7). Therefore, a stiffness reduction corresponding to each column diameter can be simulated at any level of the model (damage intensities: 6 mm – 98%., 10 mm – 85% and 12 mm- 68%).

The frame model was instrumented with accelerometers and the configurations were such that within one test series to obtain a mode shape, the sensor locations were

varied in an overlapping trend (discussed in testing procedure section) for an optimum usage of the limited number of sensors. Moreover, when designing the frames, it was ensured that the weight of the structural elements (mass per slab 1.5 kg) would be significantly higher than the weight of the sensors and the cables (9.1 g), so that the effect of sensors on the response is minimal. Threaded holes were supplied at all center points of the beam spans in all 4 directions to stud-mount the sensors, to ensure the accuracy of results (Kim et al., 2007) (Figure 4-10). The sensors are attached in respective floors to record the horizontal acceleration response along the direction of motion. It is a must to fix one sensor on the shaking table deck as a control, at all times (Figure 4-3).

Furthermore, slots were provided in all beams for rigid attachment of external masses to incorporate irregularities in to the frame model (Figure 4-11). At the initial design stage, the element masses (column attachments = 13 kg, beam attachments = 11 kg, base slab = 4 kg, connections = 1.1 kg) and the external masses (1 kg steel mass blocks up to 20 kg) were determined (Table 4-1) such that the total structural mass will not exceed the shaking table mass limit.

It should be noted that the scaling of the model does not satisfy all the similitude requirements due to the limitations imposed by the shaking table (weight limit, table dimensions). However, the geometric similitude was maintained, thereby, enabling the results to be used as a benchmark for future studies.
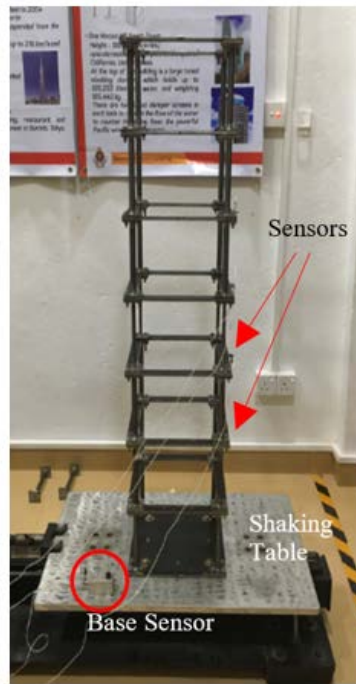
Figure 4-3- Improved framed model mounted on the shaking table with sensor arrangement for a sample test scenario

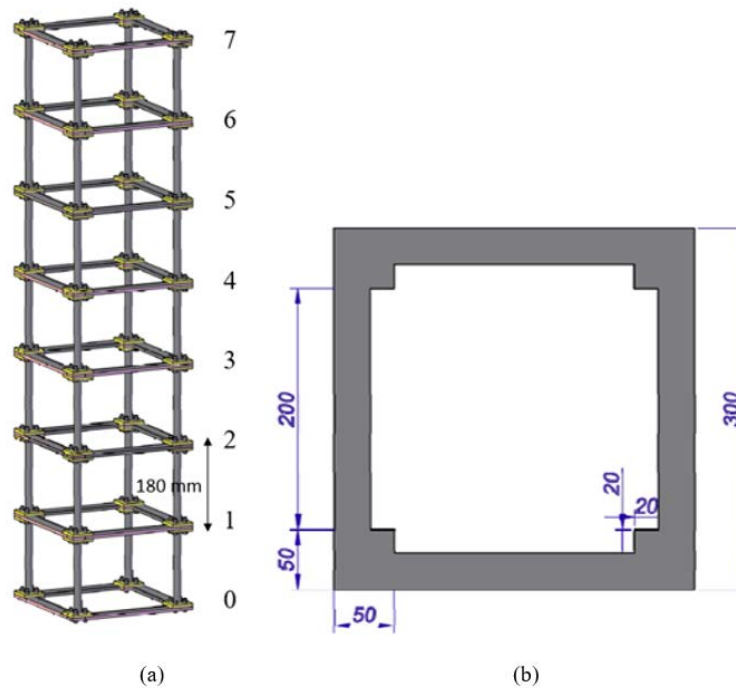(a)   (b)

Figure 4-4- Improved experimental model (geometric scale 1:20) (a) schematic diagram (b) dimensions of the steel beam arrangement (mm) (thickness = 6.35 mm)
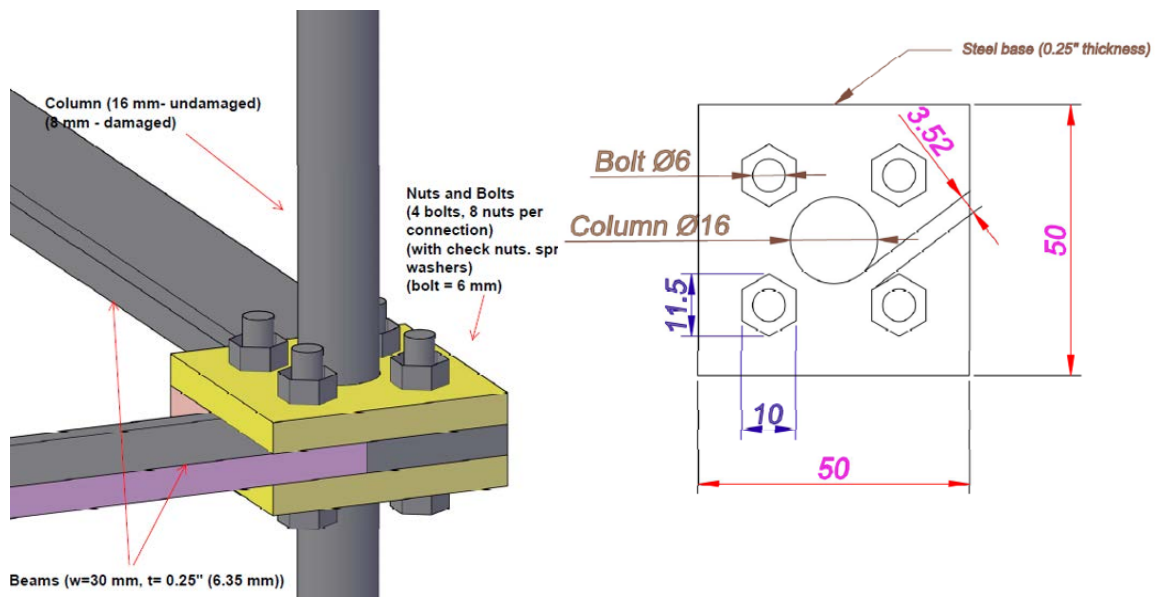
Figure 4-6- Beam-column connection detail
(3-D view)

Figure 4-5- Column connection detail
(plan view)

16 mm column

12 mm columns
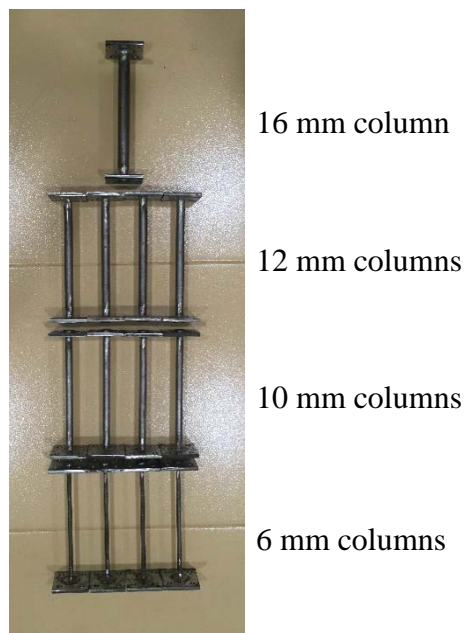
10 mm columns

6 mm columns

Figure 4-7- Column sizes to impose
damage by column stiffness
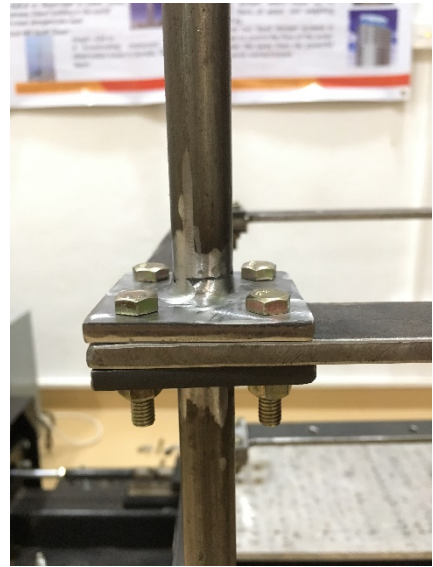reduction

Figure 4-8- Fixity at the base

Figure 4-9- Connection of a

column and beam slab

Figure 4-10- Accelerometer sensor connection to the slab using threaded holes to

ensure zero relative movement

Table 4-1 Mass calculation for the framed model

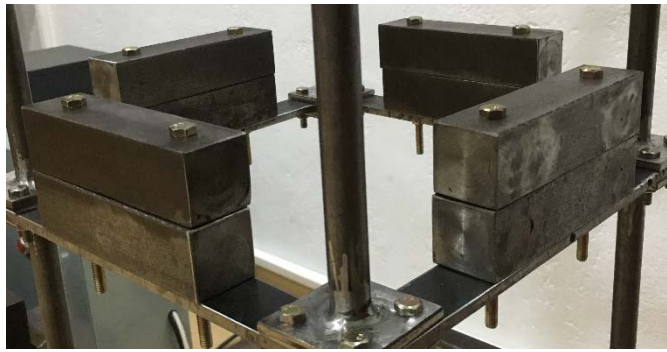| Element Type	#	Per Element Mass	Mass (kg)
Column + plates pieces	28	0.457	12.8
Slab parts	7	1.516	10.6
Base slab	1	4.012	4.0
Nuts	124	0.002	0.3
Bolts	124	0.007	0.9
Total Mass of structure			**29**

Figure 4-11- External mass attached to the framed structure for irregularity conditions

Figure 4-12- External mass blocks (1 kg per block)

4.4.1. Testing Procedure: Regular model

The main aim of the experiments was to identify the damage detection capability (Level 1 of SHM objectives) of the proposed MSS and MSC methods for a

frame structure. Therefore, damage was induced at a known location (3rd storey) and the damage magnitude was varied using the fabricated column attachments (6 mm, 10 mm, 12 mm).

Four main scenarios were tested, namely, undamaged, damaged 6 mm, 10 mm and 12 mm (Table 4-2). The damage intensity (DI) is defined for each column size. Within each scenario 8 numbers of tests were conducted according to the arrangement in Table 4-3 to facilitate systematic overlapping of 2 sensors (density of sensor results increased which is an identified requirement by the preliminary model to smoothen the mode shape). Initially in test 1 the sensors were distributed to obtain an overview response and consequently the sensors were overlapped, 2 per each test, from test 3 to test 6. Additionally, torsional response was checked for each scenario according to test 7 and test 8 in Table 4-3 ('ch' indicates the channel number the sensors are connected with).

Table 4-2- The scenarios tested for regular framed structure (Experimental model)

Scenario Number	Description
1	Undamaged
2	Damaged 3rd storey: with 6 mm columns (DI 98%)
3	Damaged 3rd storey: with 10 mm columns (DI 85%)
4	Damaged 3rd storey: with 12 mm columns (DI 68%)

Table 4-3- The test series conducted for each scenario with sensor overlapping

Test series: Regular framed		Test number							
		1	*2*	*3*	*4*	*5*	*6*	*7*	*8*
Storey number	*7*	ch1	ch1					ch1,2,3	ch1,2,3
	6		ch3	ch3					
	5	ch2	ch2	ch2	ch2				
	4			ch1	ch1	ch1			
	3				ch3	ch3	ch3		
	2	ch3				ch2	ch2		
	1						ch1		
	Base	ch0	ch0	ch0	ch0	ch0	ch0	ch0	ch0

The input for the shaking table was given using the Sweep test module, which allows the user to input a range of sine waves and adjusts its amplitudes based on the acceleration feedback from the sensors. The resonance frequency of the structure can easily be determined using the acceleration-frequency response spectrum. At the determined frequency, the amplitudes at each sensor node was calculated and mode shape was obtained using curve fitting, for all 4 scenarios (Wahab & Roeck, 1999). The process diagram for obtaining the MSS and MSC from the experimental model is shown in Figure 4-13. Furthermore, within the 8 number of tests conducted per scenario, the input range of sine sweep was reduced while including the resonance frequency, to optimize the process and limit the damage accumulation (Figure 4-14).
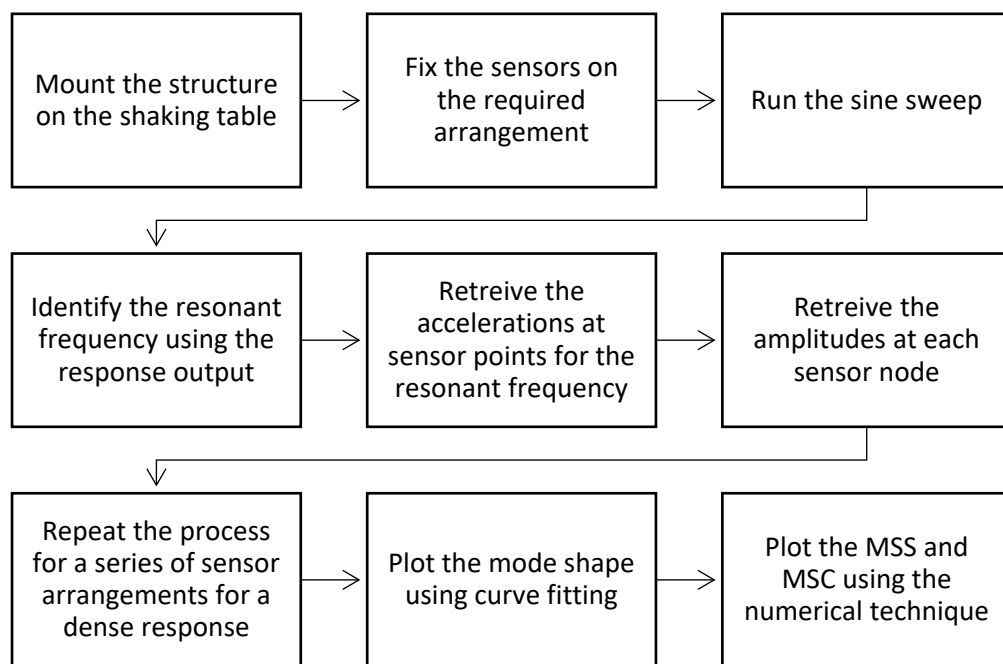

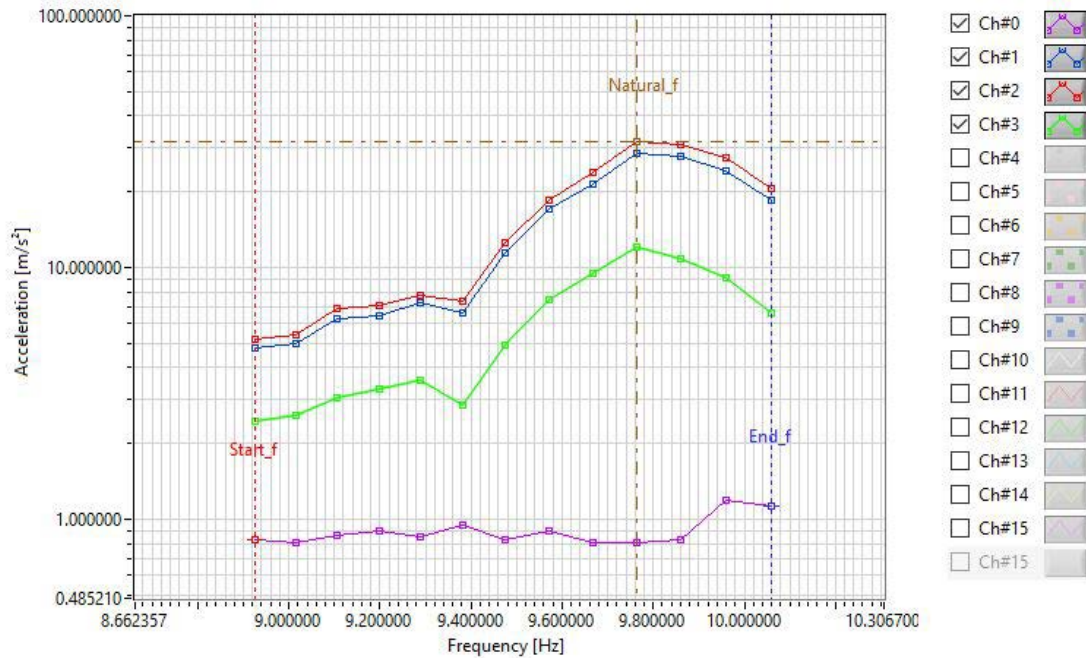Figure 4-13- Process diagram for obtaining the MSS and MSC from shaking table experiments

Figure 4-14- Reduced input range of sine sweep to prevent unnecessary damage
accumulation (between 9 Hz and 10 Hz)

4.4.1. Testing Procedure: Irregular model

Every structure is unique due to the different irregularities present. This poses a significant challenge in damage assessment strategies due to the complexity of structural behavior. Irregularity can be divided in to two main categories, vertical and plan irregularities (Hosur, 2013). Mass irregularity is included in the vertical category, which is created if a weight of a storey is more than 200% of the weight of adjacent stories in a structure (Hosur, 2013). The effect of mass irregularity on the damage detection capability using DMSS and DMSC methods were investigated for both the experimental and the FE frame model.

The features of the improved model that enables external mass attachments were utilized in this section. To match the 200% mass change criteria, the required

mass was 8 kg (8 x 1 kg masses), which is greater than twice the mass per storey (3.34 kg). Masses were rigidly fixed on the 3rd storey to create the irregularity and the same test procedure was carried out to obtain the mode shape. From the comparison between regular and irregular mode shape derivatives the DMSS and DMSC were obtained.

Figure 4-15 Mass irregularity imposed on the 3rd storey in the experimental model, mounted on the shaking table

CHAPTER V

5. FINITE ELEMENT MODEL

5.1. Undamaged Model

A FE model was developed for the improved experimental test model using the SAP2000 software package. The dimensions were the same. Shell thin elements were used for the slab plate and circular frame elements were used for the columns. Properties of steel were given for the material definition (Modulus of elasticity = 210 GPa, density = 76.9 kN/m^3, Poisson's ratio = 0.3). The connection nodes of base slab to the shaking table were fixed and body constraints were assigned. The optimum discretization for a column was determined by checking the convergence of the resonance frequency for a range of discretization and 56 parts per column were selected (Figure 5-2). A modal analysis was performed for the undamaged model and the modal frequency results are given in Figure 5-3. The resonance frequency for the 1st translational mode (1st mode) was obtained (12.17 Hz), which is only 0.2% different than that of the experimental model (12.15 Hz). The slight difference might be due to the modelling of the rigidity of bolted connections and the non-linearity of the experimental model. However, since the deviation is within 25% the model can be sufficiently validated (CSI, 2017). Hence, this FE model was used for the parametric analysis by inducing damage at required stories and magnitudes. The frequency for 2nd mode (translational) and the 3rd mode (torsional) were not captured in the experimental model due to the limitations of 1-DOF and maximum frequency.
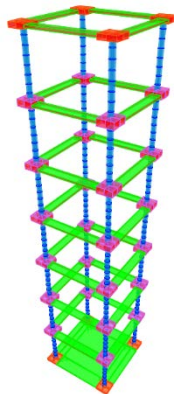

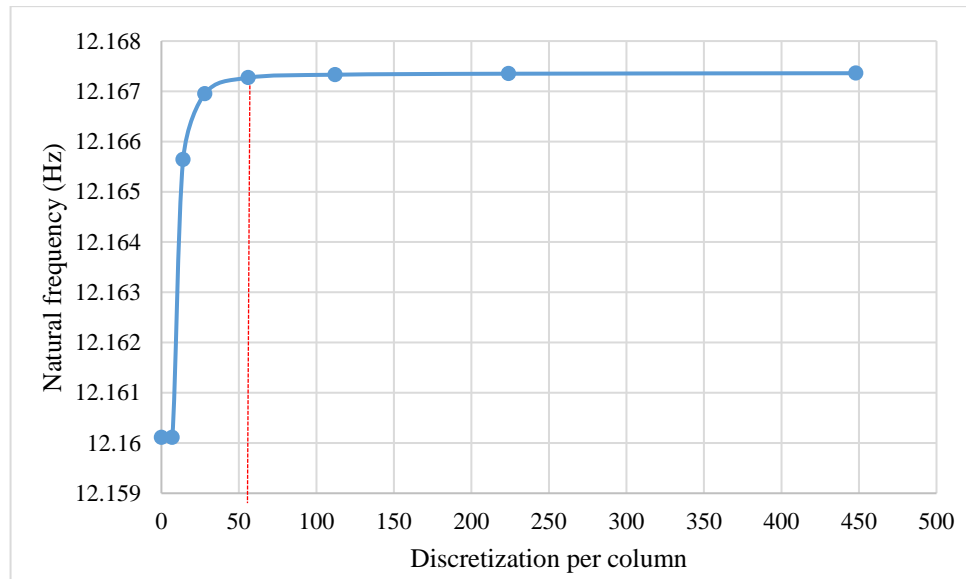Figure 5-1 Finite element model for the undamaged structure

Figure 5-2- Selection of the optimum number of discretization based on the resonant frequency
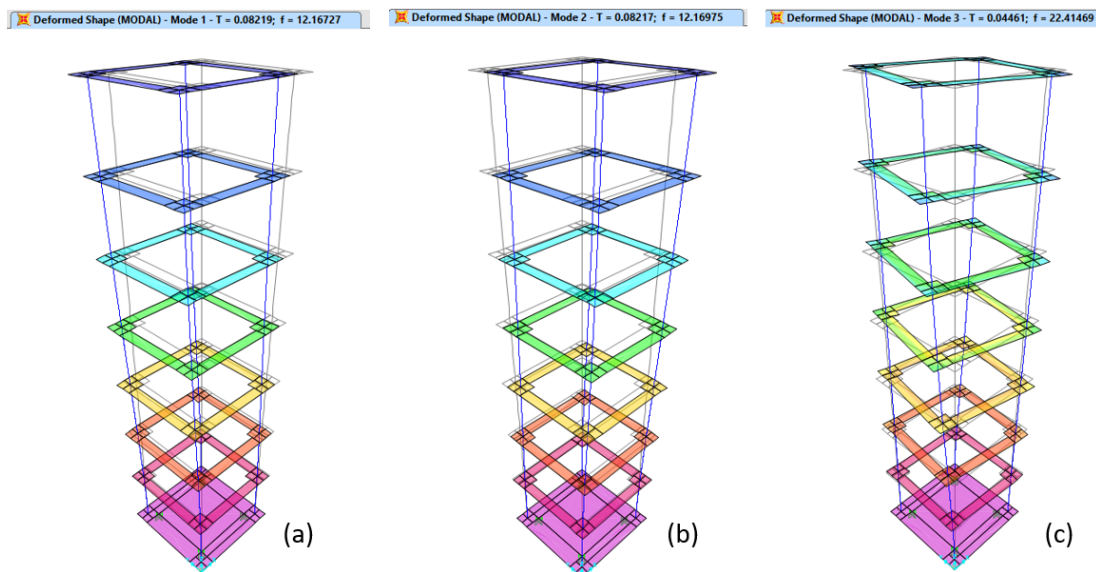

Figure 5-3- Undamaged framed model mode shapes for (a) mode 1 (translational, f = 12.17 Hz) (b) mode 2 (translational, f = 12.17 Hz) (c) mode 3 (torsional, f =22.42 Hz)

5.2.   Damaged Model

Damage was induced using column stiffness reduction by assigning smaller cross sectional areas for the frame elements. Two main aspects, localization and severity were analyzed. The modal analysis results were used to obtain the modal

frequencies and mode shapes, from which DMSS and DMSC for undamaged and damaged models were plotted.

5.2.1. Damage localization

Damage was induced in single locations for all the stories (from base storey to 6th storey) and the 3 damage scenarios (6 mm, 10 mm, 12 mm) tested in the shaking table were used. Therefore, all together 21 cases were compared with the undamaged response.

Table 5-1- The scenarios tested for regular framed structure: Damage on different storeys (Finite Element model)

Scenario Number	Description
1	Undamaged
2	Damaged 0-6th storeys: with 6 mm columns (DI 98%)
3	Damaged 0-6th storeys: with 10 mm columns (DI 85%)
4	Damaged 0-6th storeys: with 12 mm columns (DI 68%)

5.2.2. Damage severity

Damage intensity was varied from 98% to 0.5% and was induced on the 3rd storey (identified as the location with optimum damage identification capability from the damage localization analysis).

5.3. Irregular Model

Mass is modified in the beam areas of the shell elements to simulate a similar mass irregularity (mass modifier = 8.41) for each storey. The model for the 3rd storey mass irregularity was verified with the experimental model using modal frequencies. The frequencies, DMSS and DMSC were plotted to investigate the behavior.

CHAPTER VI

6. RESULTS AND DISCUSSION

6.1. Results of the Regular Experimental Model

MSS and MSC were obtained from the mode shapes (using equation (2) - (7)) of the 4 scenarios and the differences between the undamaged and the 3 damage cases were plotted. For ease of comparison, the plots were normalized. For reference Figure 6-1 shows the normalized mode shapes for the undamaged and the 6 mm damage scenarios. Figure 6-2 shows the plots for DMSS and DMSC for all 3 damage scenarios.

The resonance frequencies obtained for undamaged, damaged 12 mm, 10 mm and 6 mm are 12.15 Hz, 12.03 Hz, 11.80 Hz and 9.76 Hz. The resonance frequencies decrease with the increase of the damage intensity. The DMSS shows a maximum value between 3rd and 4th stories, for the 6 mm and the 10 mm damage cases (Figure 6-2 (a) and (b)). The magnitude of the maximum point shows a decrement when the damage intensity is lowered. The DMSC for the 6 mm and the 10 mm cases, show a zero-crossing between 3rd and 4th stories. But the magnitude difference between the two consecutive points, on either sides of the zero crossing shows a decrement when the damage intensity is lowered. However, in the 12 mm damage case, which has the lowest damage intensity from the 3 cases, the expected trends are not visible (Figure 6-2 (c)). This might be due to the experimental errors or the effect of unavoidable damage accumulation, which provides an indication that this method shows discrepancies when trying to detect damages with low intensities.

The experimental shaking table tests suggest that this method sufficiently detects damages induced in a mid storey of a regular steel frame structure if the damage intensity is high. Henceforth, a parametric analysis was performed using a FE model to probe in to the aspects of damage localisation and damage severity.
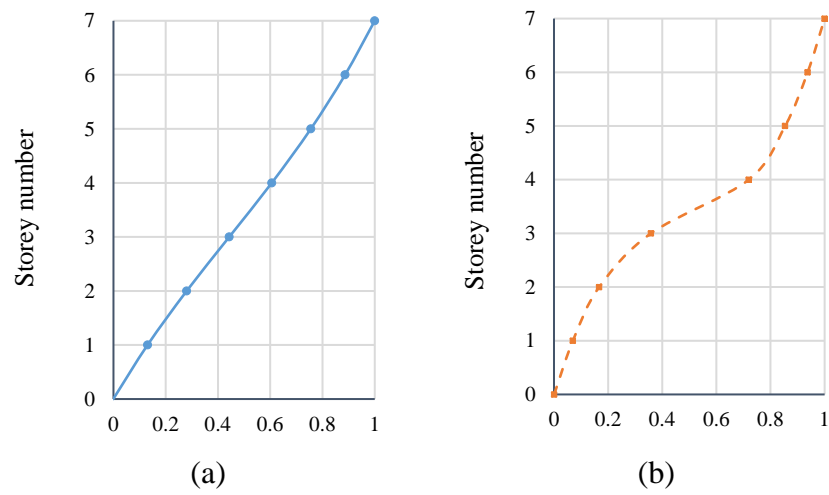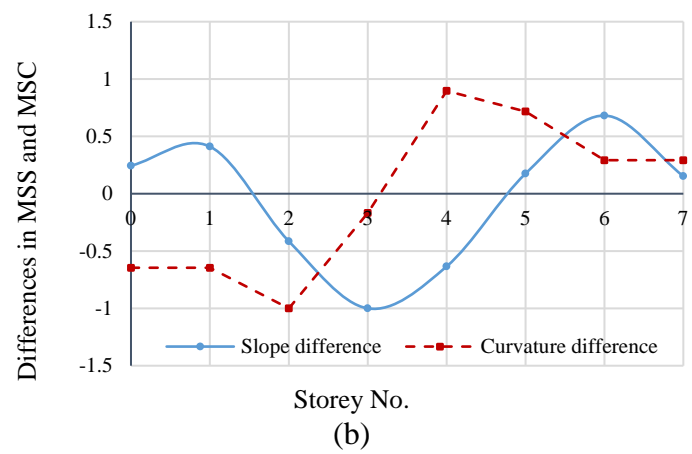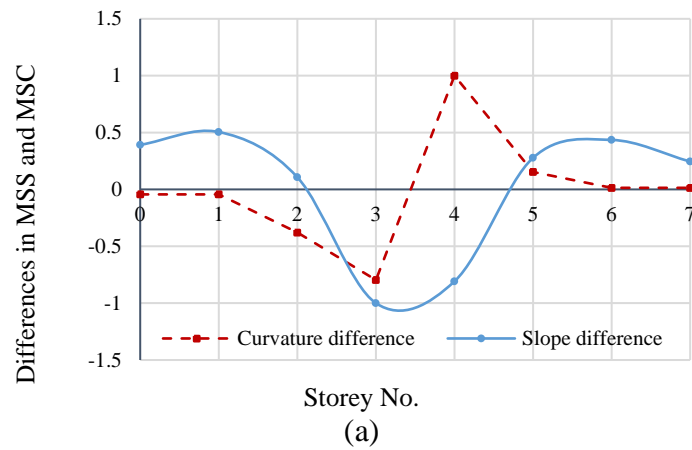
Figure 6-1 Normalized mode shapes of (a) undamaged structure and (b) damaged structure (for 6 mm damage scenario)

(a)

(b)

1.5

1

0.5

0

-0.5

-1

-1.5

0   1   2   3   4   5   6   7

Differences in MSS and MSC

Slope difference   Curvature difference
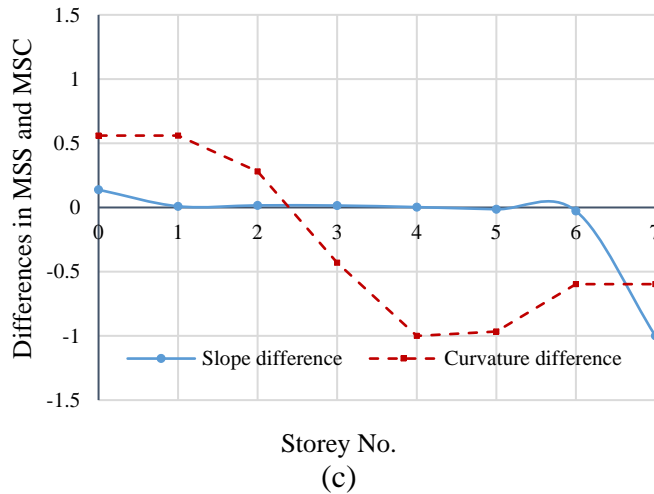
Storey No.

(c)

Figure 6-2- Difference in mode shape slopes (DMSS) and differences in mode shape curvatures (DMSC) for (a) 6 mm damage scenario (9.76 Hz) (b) 10 mm damage scenario (11.80 Hz) (c) 12 mm damage scenario (12.03 Hz), for damages induced in columns between 3rd and 4th storeys

6.2. Results of the Parametric Analysis using Finite Element Regular Model
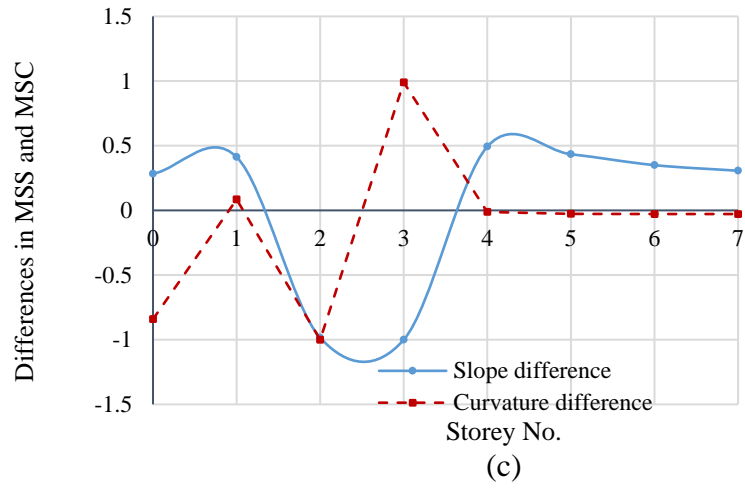
6.2.1. Damage localization

Figure 6-3 shows the plots of the differences of mode shape derivatives for the 6 mm damage scenario. The method used for damage detection is similar to what was used in the experimental analysis. Both the DMSS and DMSC accurately indicate the location of damage for the middle stories (2nd, 3rd, 4th and 5th). As for the boundary stories (base and 6th) only the DMSS shows a maximum value and the DMSC fails to indicate damage. Additionally, for the damage at 1st storey, the DMSS indicates the correct location and DMSC, a false location (between base and 1st). The usage of backward difference and forward difference methods (equations (2) – (7)) for obtaining the boundary values seems to be the underlying cause for this behavior. In order to investigate this effect, the same analysis was repeated only using the central difference method. The results for all 3 damage scenarios (damage intensity % (DI%) relevant to reduction of stiffness) with and without incorporating the backward and forward difference methods are tabulated in Table 6-1 and Table 6-2 respectively. The legend defines the damage localization capability.

As identified before, damage localization accuracy is higher for high damage intensities (corresponds with experimental results). DMSS shows better detectability at boundaries than the DMSC (Table 6-1) while forward and backward method is incorporated.

Eliminating forward and backward difference methods increase the detectability at 1st and 5th stories for both DMSS and DMSC, from which DMSC shows a significant improvement for 1st storey. Nonetheless, data is not available for boundary stories (base and 6th). Furthermore, DMSC shows a slightly better detectability compared with DMSS, when only the central difference method is used (Table 6-2).

Overall, damage localization accuracy increases when only the central difference method is used for middle stories other than the two boundaries.

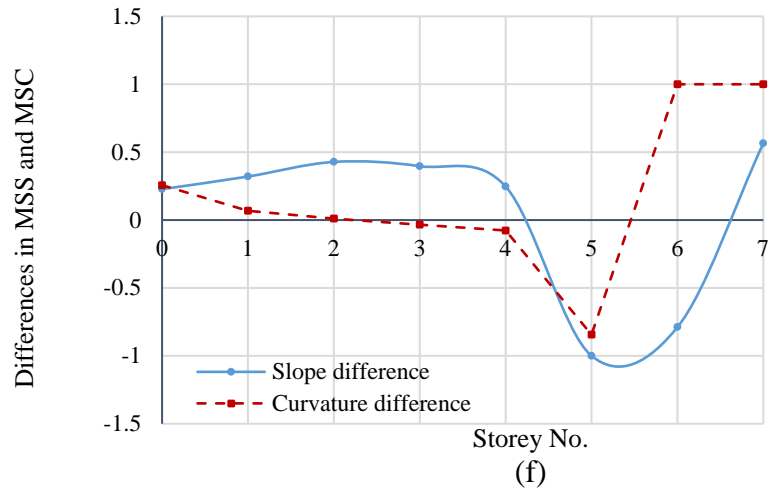

(a)

(b)

(c)

(d)

(e)

34

(f)

(g)
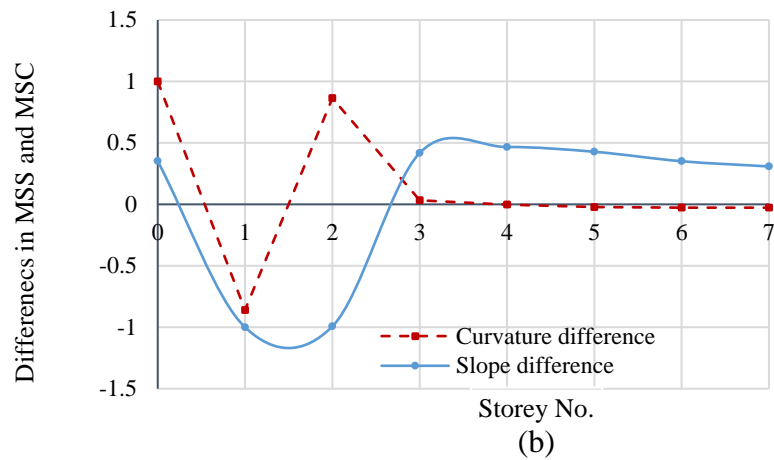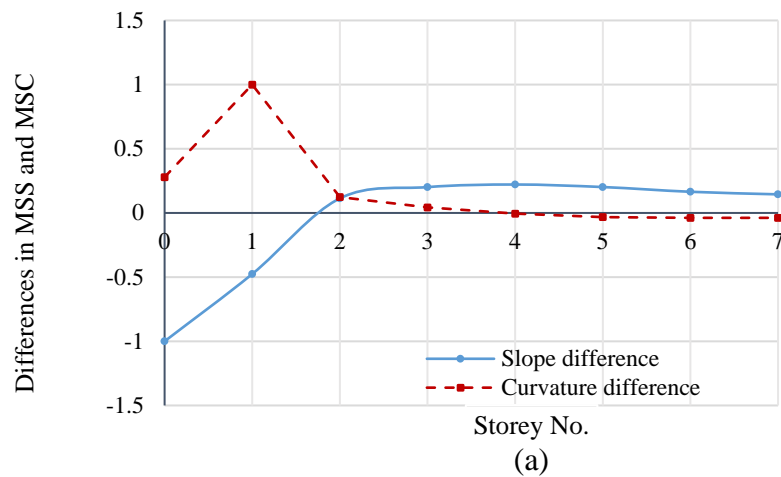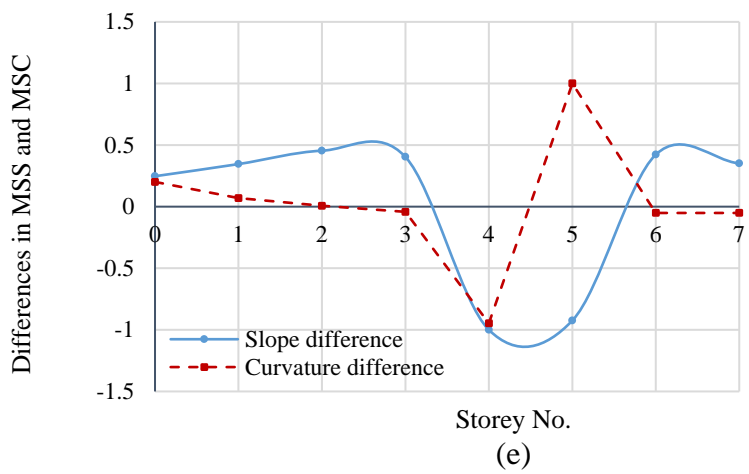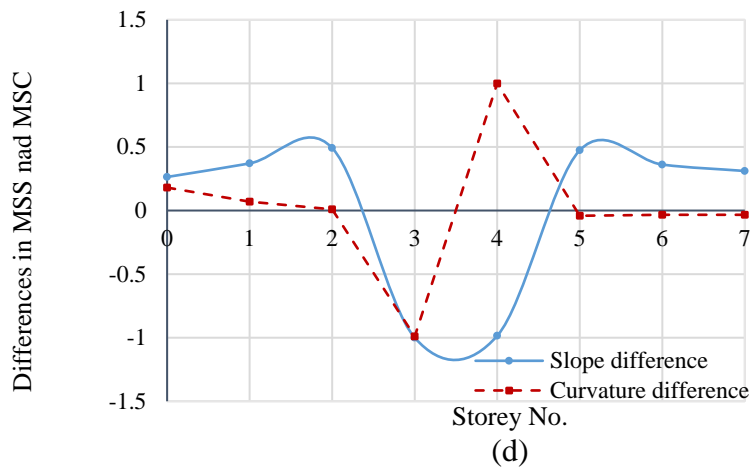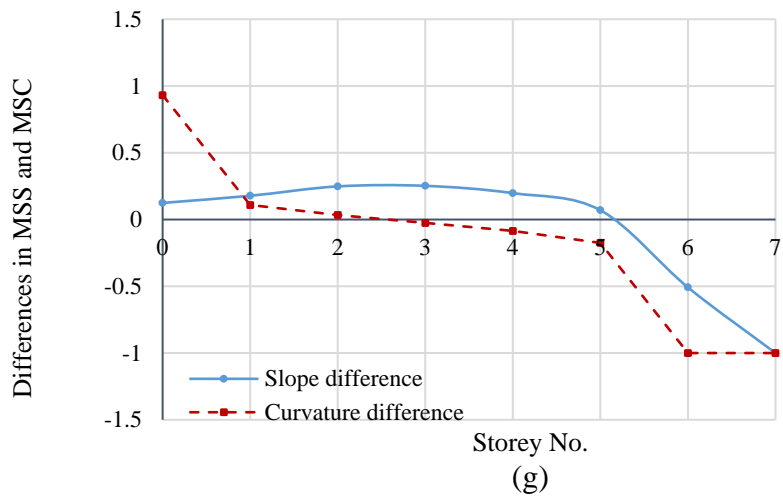
Figure 6-3- Difference in mode shape slopes (MSS) and mode shape curvatures (MSC) for 6 mm damage scenario induced at (a) base storey (b) 1st storey (c) 2nd storey (d) 3rd storey (e) 4th storey (f) 5th storey (g) 6th storey

Table 6-1- Damage localisation capability (forward and backward difference method incoportaed)

| Damage localization matrix		Damage scenario (DI%)					
		DMSS			DMSC		
		6 mm (98%)	10 mm (85%)	12 mm (68%)	6 mm (98%)	10 mm (85%)	12 mm (68%)
Damaged storey	0f						
	1f						
	2f						
	3f						
	4f						
	5f						
	6f						

Legend
▨ Identified on exact location
▨ Identified in a larger range (damage location included)
▨ Identified in a nearby range (damage location not included)
▨ False location

Table 6-2- Damage localisation capability (forward and backward difference method eliminated)

Damage localization matrix		Damage scenario (DI%)					
		DMSS			DMSC		
		6 mm (98%)	10 mm (85%)	12 mm (68%)	6 mm (98%)	10 mm (85%)	12 mm (68%)
Damaged storey	0f	–			–		
	1f						
	2f						
	3f						
	4f						
	5f						
	6f	–			–		

Legend
▨ Identified on exact location
▨ Identified in a larger range (damage location included)
▨ Identified in a nearby range (damage location not included)
▨ False location

6.2.2. Damage severity

The modal frequencies, DMSS and DMSC were obtained for the tested damage intensities. Figure 6-4 shows the normalized difference of modal frequencies between the undamaged and damaged models. It is evident that a significant difference can only be identified after 85% damage. Therefore, as discussed in the introduction modal frequency is not a reliable damage detection tool (Peter Cawley, 2018)(Doebling et al., 1998)(Fan & Qiao, 2011).
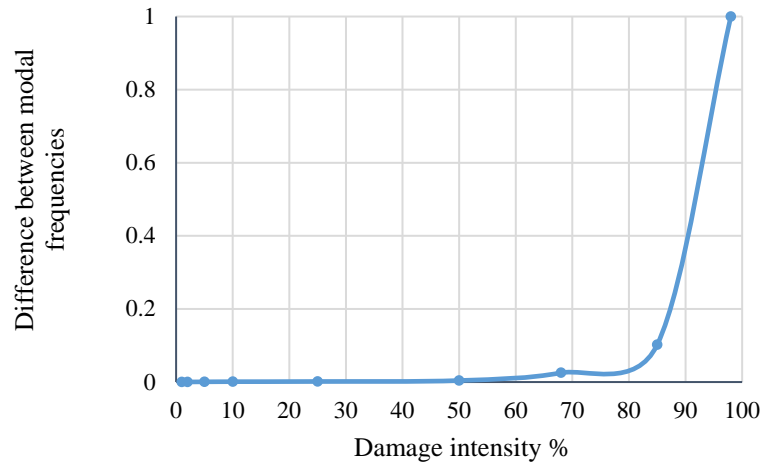

Figure 6-4- Normalized differences of modal frequencies between undamaged and damaged models vs damage intensity %

The aim of this section was to investigate in to the relationship between the damage severity and the mode shape derivatives. From the experimental analysis it was identified that with the variation of damage severity, the absolute maximum value of DMSS and, absolute difference between maximum and minimum DMSC values, change. Therefore, normalized values of the above parameters for a variation of damage intensity % was plotted (Figure 6-5). The parameter obtained from DMSC shows a higher sensitivity than the parameter from DMSS. The DMSS parameter shows an approximately constant value up to 68% intensity and gradually starts to increase afterwards, whereas the DMSC parameter shows an increasing trend with the increasing intensity.
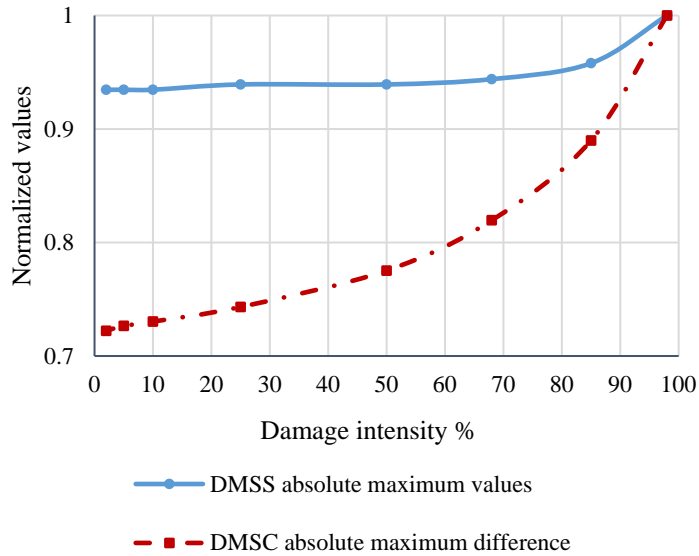
Figure 6-5- Normalized values for the absolute maximum
values of DMSS and absolute maximum difference of
DMSC vs damage intensity %

6.3. Results of the Irregular Model

6.3.1. Results of irregular experimental model

The DMSS shows a maximum value between 1st and 2nd storeys (Figure 6-6) and the DMSC shows a maximum jump between the same storeys (Figure 6-7). Therefore, this method yields a false detection of damage between the 1st and 2nd stories for the experimental model. Which suggests that a mass irregularity in a specific storey can significantly affect the DMSS and DMSC methods.
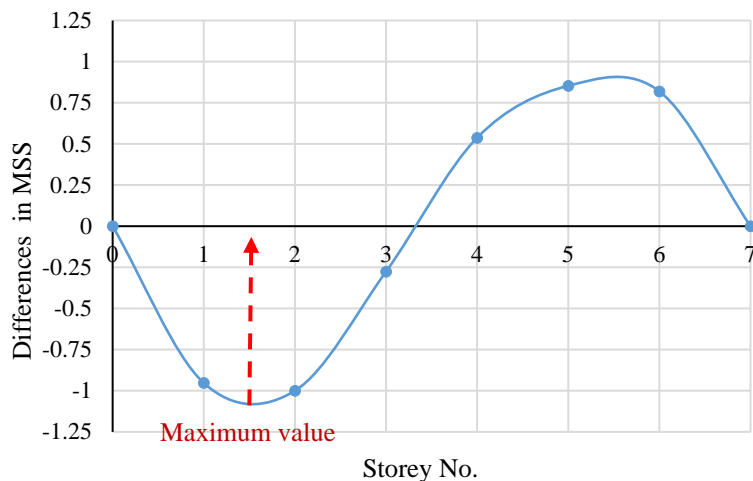

Figure 6-6- Difference in mode shape slopes (DMSS) between the regular and
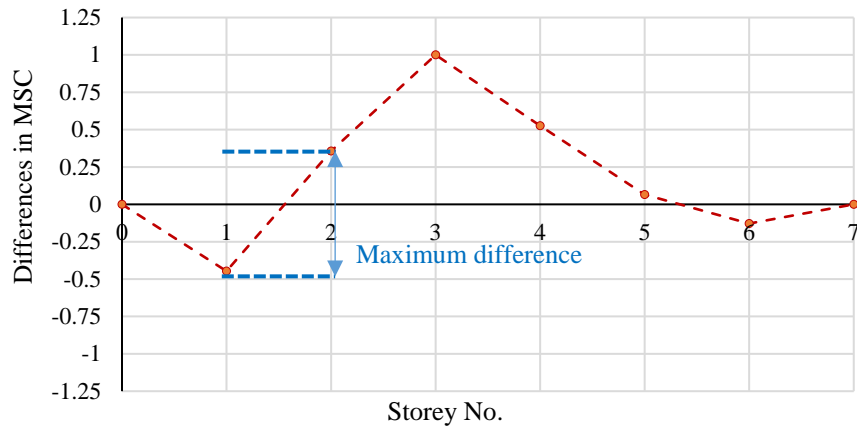irregular model (mass irregularity induced at 3rd storey)

Figure 6-7- Difference in mode shape curvatures (DMSC) between the regular and irregular model (mass irregularity induced at 3rd storey)

6.3.2. Results of irregular finite element model

The effect of mass irregularity was further investigated by varying the irregularity location in the FE model. In comparison with the regular model, the resonance frequencies decreases with the incorporation of mass irregularity and shows a higher difference when masses occur in the higher stories (Figure 6-8). Hence, it is evident that the mass variations affect the resonance frequencies and using it alone for damage detection can be faulty.
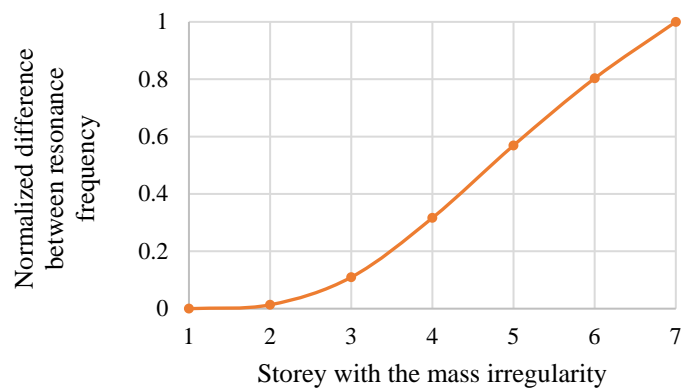

Figure 6-8- Normalized differences between resonance frequencies of a regular and irregular frame vs storey with the mass irregularity

Furthermore, the DMSS and the DMSC variations resulted in false damage localization as well. Table 6-3 shows the detected locations as opposed to mass irregularity stories.

Table 6-3- False damage detection for mass irregularities at each storey

Mass irregular storey	False damage detected storey	
	DMSS	*DMSC*
0f	At 4th	4th-5th
1f	At 1st	4th-5th
2f	1st-2nd	1st-2nd
3f	1st-2nd	1st-2nd
4f	5th-6th	5th-6th
5f	5th-6th	3rd-4th
6f	5th-6th	5th-6th

Therefore, it is paramount to monitor the mass flow in order to prevent false damage detection as it affects the MSS and MSC. The undamaged state need to be updated if a significant mass irregularity occurs in a structure.

CHAPTER VII

7. CONCLUSIONS AND FUTURE WORK

On assessment of damage using the MSS and MSC for the 6-storey steel frame experimental and a FE model, following conclusions can be derived,

7.1. Damage localization

Damage detection capability reduces at boundaries and when damage intensity is low. DMSS shows better detectability at boundaries than the DMSC (Table 6-1) while forward and backward method is incorporated. However, when forward and backward method is removed detectability of 1st and 5th storeys significantly increase for both the methods (Table 6-2). Therefore, with only the central difference method accurate damage detection can be done for the mid floors (but not for boundaries).

7.2. Damage severity

Damage is identifiable from frequency reduction only after 85% of damage intensity. Damage severity can be quantified using two parameters related to DMSS and DMSC and it was identified that DMSC is more sensitive to damage than DMSS.

7.3. Mass irregularity

In comparison with the regular model, the resonance frequencies had decreased with the incorporation of mass irregularity and shows a higher difference when masses occur in the higher stories. Mass flow can result in fault detection of damage. Hence, monitoring of mass flow should be implemented when applying to full scale structures.

7.4. Future work

Furthermore, using the improved experimental model multiple damage situations and plan irregularity effects can be investigated for an enhanced understanding on the damage detection capability of the mode shape derivatives based method. Nonetheless, prior to implementing this approach on real-scale structures numerous complexities such as structural irregularities, operational and environmental

varying conditions, multi-disciplinary nature of technology required and the sensitivity of sensor networks should be methodically addressed in the future extensions of this study.

REFERENCES

Altunışık, A. C., Okur, F. Y., Karaca, S., & Kahya, V. (2019). Vibration-based damage detection in beam structures with multiple cracks: modal curvature vs. modal flexibility methods. *Nondestructive Testing and Evaluation*, *34*(1), 33–53. https://doi.org/10.1080/10589759.2018.1518445

Beskhyroun, S., Oshima, T., Mikami, S., & Tsubota, Y. (2006). Damage identification of steel structures based on changes in the curvature of power spectral density. In *2nd International conference on structural health monitoring of intelligent infrastructure* (pp. 11–21).

Brownjohn, J. M. W. (2006). Structural health monitoring of civil infrastructure. *Philosophical Transactions of The Royal Society A*, *365*(1851), 589–622. https://doi.org/10.1098/rsta.2006.1925

Cawley, P. (2018). Structural health monitoring : Closing the gap between research and industrial deployment. *Structural Health Monitoring*, *17*(5), 1225–1244. https://doi.org/10.1177/1475921717750047

Cawley, P., & Adams, R. D. (1979). The location of defects in structures from measurements of natural frequencies. *Journal of Strain Analysis*, *14*(2), 49–57.

Chen, H.-P., & Ni, Y.-Q. (2018). *Structural Health Monitoring of Large Civil Engineering Structures*. *John Wiley & Sons*.

CSI. (2017). *Software Verification Examples*. Computers & Structures, Inc., 1978-2017.

Dance user's guide (2016) Version 632.1. ANCO Engineers, INC.

Dessi, D., & Camerlengo, G. (2015). Damage identification techniques via modal curvature analysis : Overview and comparison. *Mechanical Systems and Signal Processing*, *52–53*, 181–205. https://doi.org/10.1016/j.ymssp.2014.05.031

Doebling, S. W., Farrar, C. R., & Prime, M. B. (1998). A Summary Review of Vibration-Based Damage Identification Methods. *The Shock and Vibration Digest*, *30*(2), 91–105.

Fan, W., & Qiao, P. (2011). Vibration-based damage identification methods: A review and comparative study. *Structural Health Monitoring*, *10*(1), 83–111. https://doi.org/10.1177/1475921710365419

Farrar, C. R., & Worden, K. (2007). An introduction to structural health monitoring. *Philosophical Transactions of The Royal Society A*, *365*, 303–315. https://doi.org/10.1007/978-3-7091-0399-9_1

Gong, M. S., Xie, L., & Ou, J. P. (2008). Modal parameter identification of structure model using shaking table test data. In *14th World Conference on Earthquake Engineering, Beijing, China*. https://doi.org/10.1109/CISP.2010.5646395

Gürkan, K., Gürkan, G., & Dindar, A. A. (2018). Design and realization of multi-channel wireless data acquisition system for laboratory-scale experiments on structural health monitoring. *Journal of Measurements in Engineering*, *6*(1), 64–73. https://doi.org/10.21595/jme.2018.19699

Hosur, V. (2013). *Earthquake-resistant design of building structures*. *Wiley*.

Kaloop, M. R., & Hu, J. W. (2016). Damage Identification and Performance Assessment of Regular and Irregular Buildings Using Wavelet Transform Energy. *Advances in Materials Science and Engineering*, *2016*, 1–11. https://doi.org/10.1155/2016/6027812

Kim, S.-E., Lee, D.-H., & Ngo-Huu, C. (2007). Shaking table tests of a two-story unbraced steel frame. *Journal of Constructional Steel Research*, *63*(3), 412–421. https://doi.org/10.1016/j.jcsr.2006.04.009

Ostachowicz, W. ;, Radzienski, M. ;, Cao, M. ;, & Xu, W. ; (2018). Novel techniques for damage detection based on mode shape analysis. In *Vibration-Based Techniques for Damage Detection and Localization in Engineering Structures* (pp. 173–196). World Scientific. https://doi.org/https://doi.org/10.1142/q0145

Pandey, A. K., Biswas, M., & Samman, M. M. (1991). Damage Detection from Changes in Curvature Mode Shape. *Journal of Sound and Vibration*, *145*(2), 321–332.

Roy, K. (2017). Structural Damage Identification Using Mode Shape Slope and Curvature. *Journal of Engineering Mechanics*, *143*(9), 04017110. https://doi.org/10.1061/(ASCE)EM.1943-7889.0001305

Roy, K., & Ray-chaudhuri, S. (2013). Fundamental mode shape and its derivatives in structural damage localization. *Journal of Sound and Vibration*. https://doi.org/10.1016/j.jsv.2013.05.003

Rytter, A. (1993). Vibrational Based Inspection of Civil Engineering Structures. *Fracture and Dynamics*, *R9314*(44).

Wahab, M. M. A., & Roeck, G. De. (1999). Damage detection in bridges using modal curvatures : application to a real damage scenario. *Journal of Sound and Vibration*, *226*(2), 217–235.

Wu, D., Yamazaki, Y., Sawada, S., Sakata, H., & Asce, M. (2018). Shaking Table Tests on 1 = 3-Scale Model of Wooden Horizontal Hybrid Structure, *144*(2017), 1–17. https://doi.org/10.1061/(ASCE)ST.1943-541X.0002115.

Ye, J., & Jiang, L. (2018). Simplified analytical model and shaking table test validation for seismic analysis of mid-rise cold-formed steel composite shear wall building. *Sustainability*, *10*(9), 3188. https://doi.org/10.3390/su10093188

Zhu, H., Li, L., & He, X. (2011). Damage detection method for shear buildings using the changes in the first mode shape slopes. *Computers and Structures*, *89*, 733–743. https://doi.org/10.1016/j.compstruc.2011.02.014

APPENDICES

Appendix A: Finite Element Model Results for 10 mm and 12 mm damage scenarios for forward and backward difference method incorporated
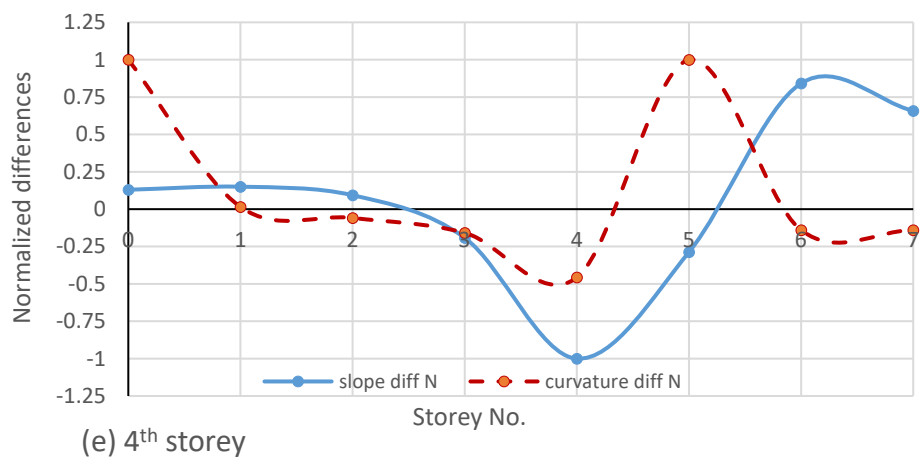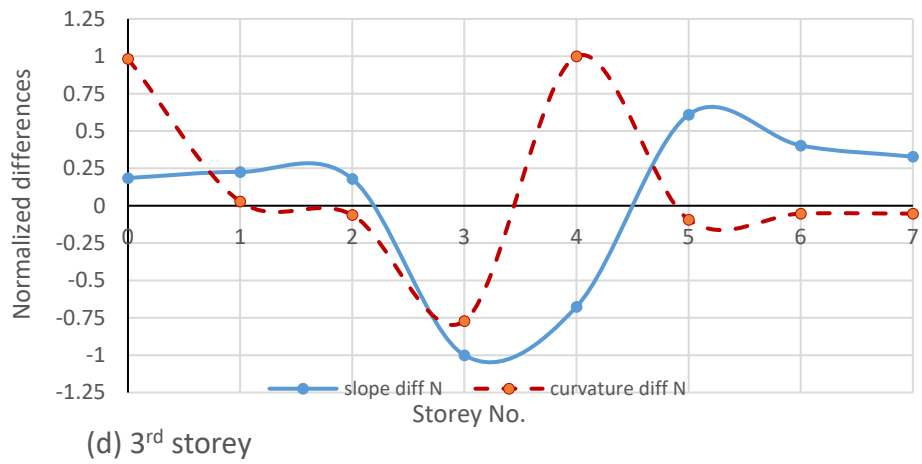
10 mm Damage Scenario

Figure A1- Difference in mode shape slopes (MSS) and mode shape curvatures (MSC) for **10 mm damage scenario** induced at (a) base storey (b) 1st storey (c) 2nd storey (d) 3rd storey (e) 4th storey (f) 5th storey (g) 6th storey


(a) base storey

(b) 1st storey

(c) 2nd storey

(d) 3rd storey

(e) 4th storey

46
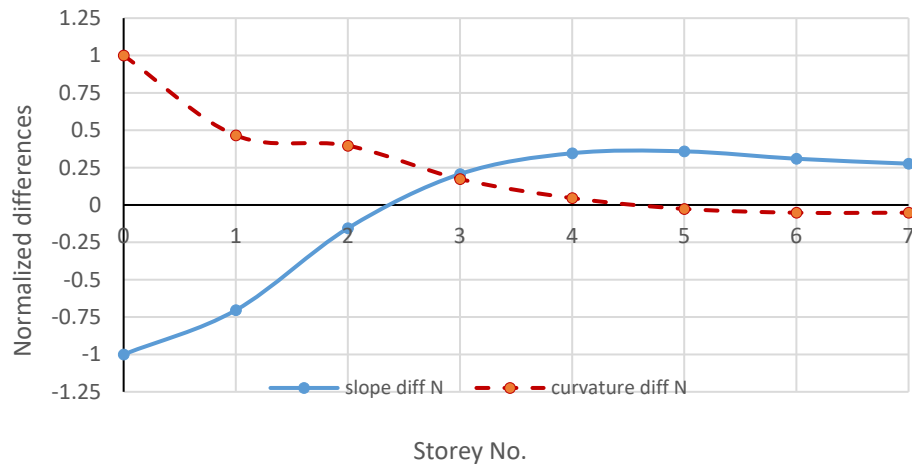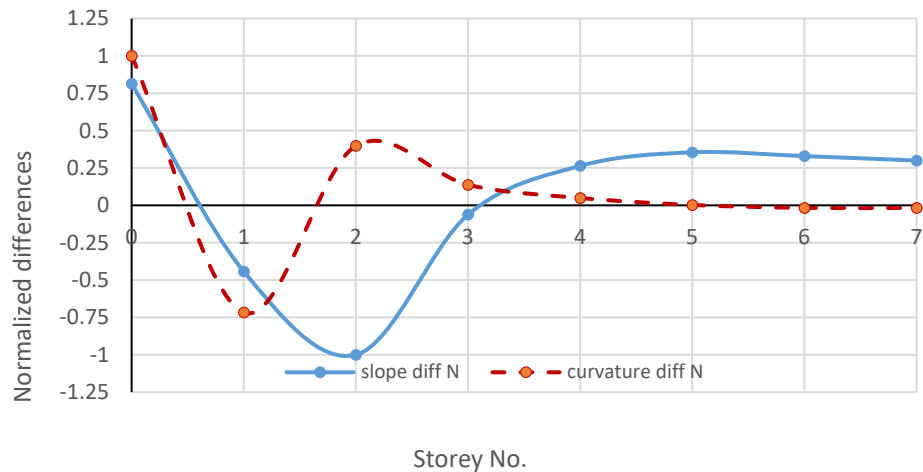
(f) 5th storey
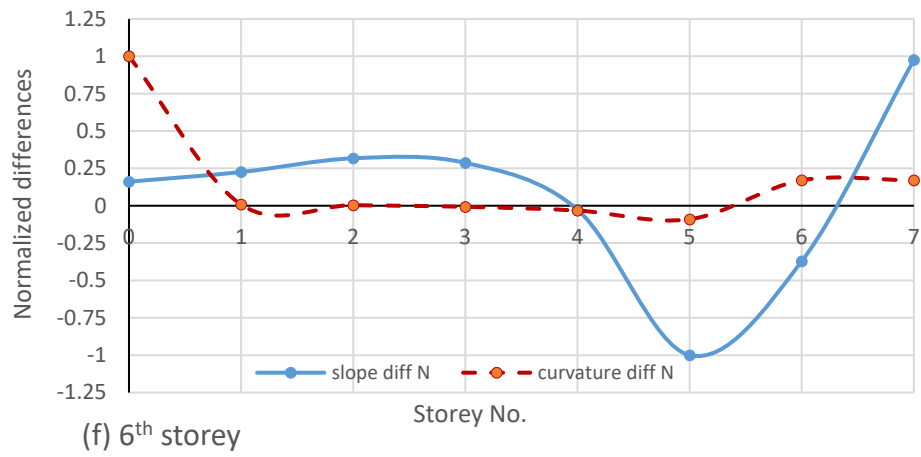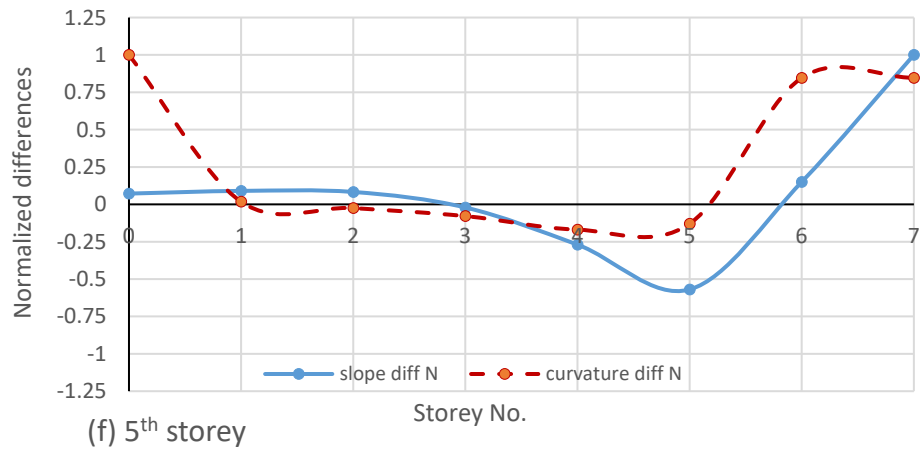
(f) 6th storey

12 mm Damage Scenario

Figure A2- Difference in mode shape slopes (MSS) and mode shape curvatures (MSC) for **12 mm damage scenario** induced at (a) base storey (b) 1st storey (c) 2nd storey (d) 3rd storey (e) 4th storey (f) 5th storey (g) 6th storey

(a) Base storey

(b) 1st storey

(c) 2ⁿᵈ storey

(d) 3ʳᵈ storey

(e) 4ᵗʰ storey

49
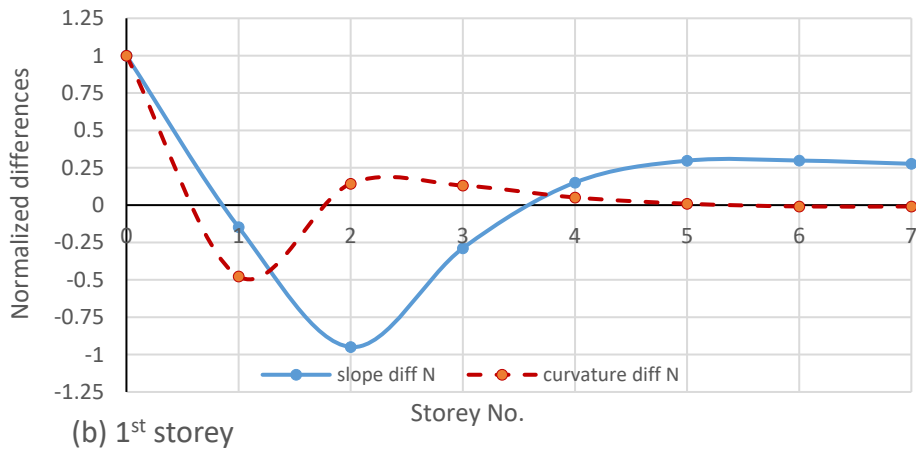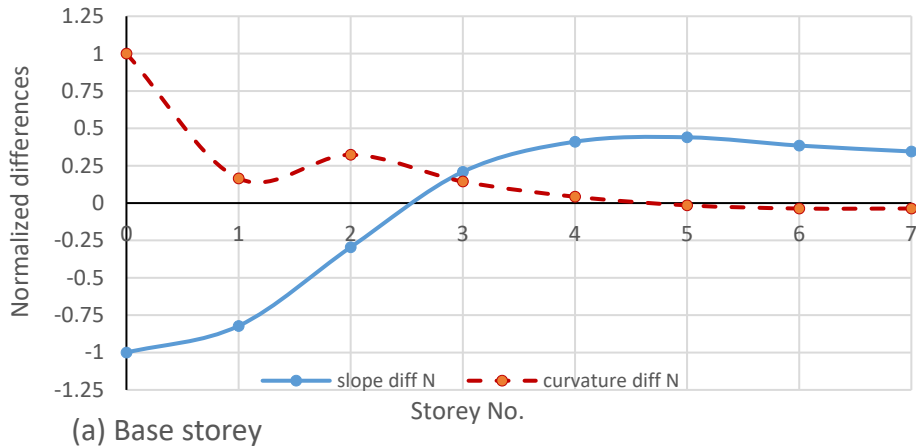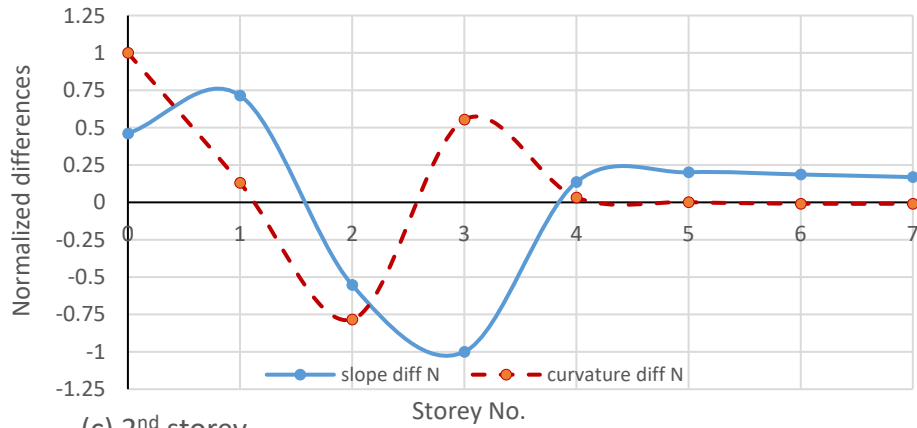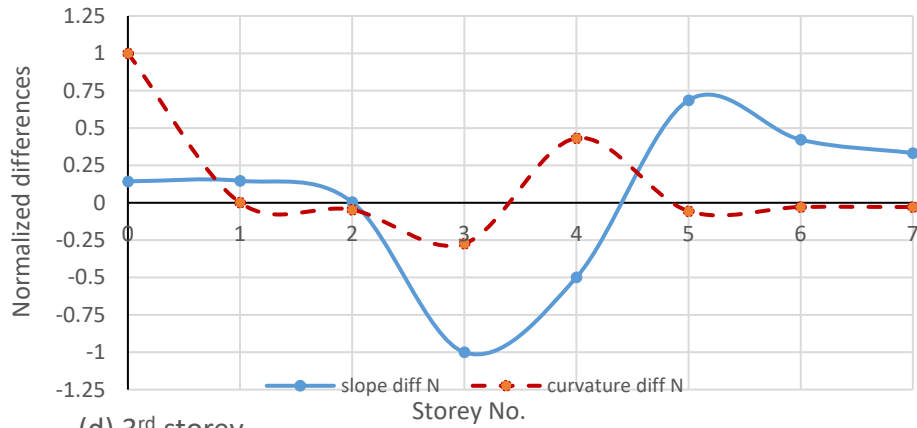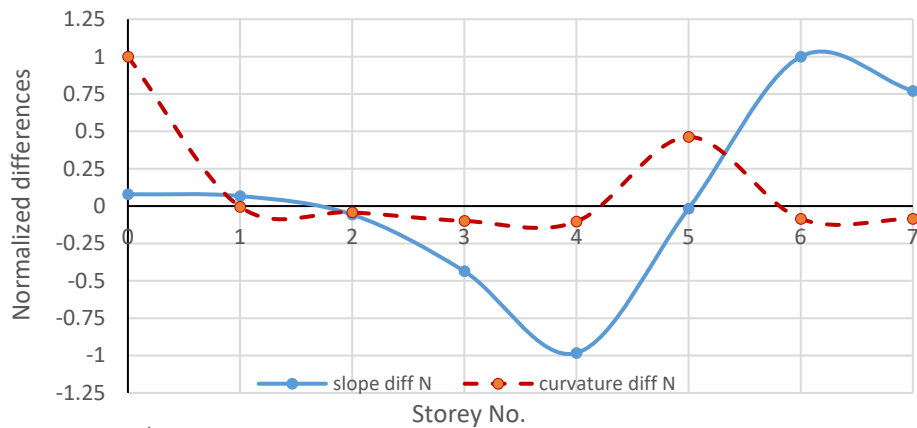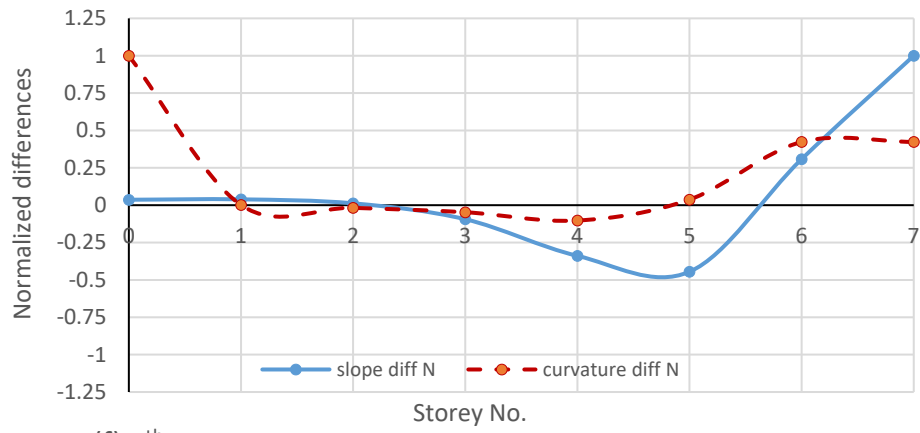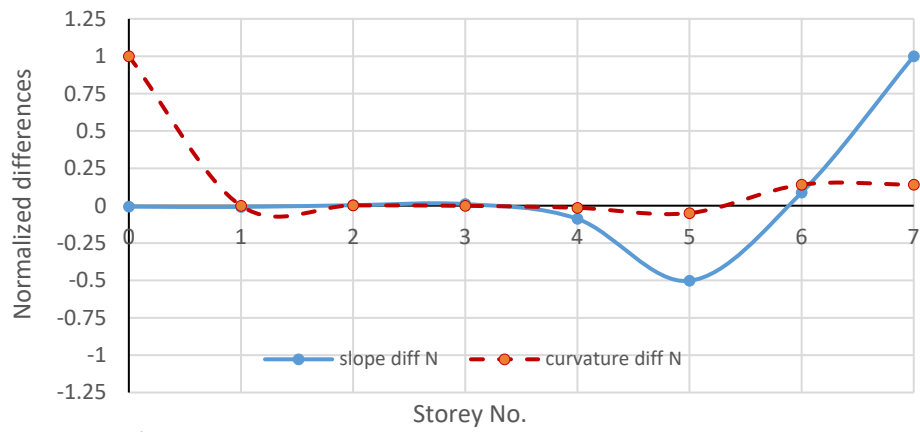
(f) 5th storey

(g) 6th storey

Appendix B: Finite Element Model Results for mass irregular model

The finite element model was used to change the mass at each level and induce mass-irregularity. The finite element model with the mass modification for 3rd storey is as follows,
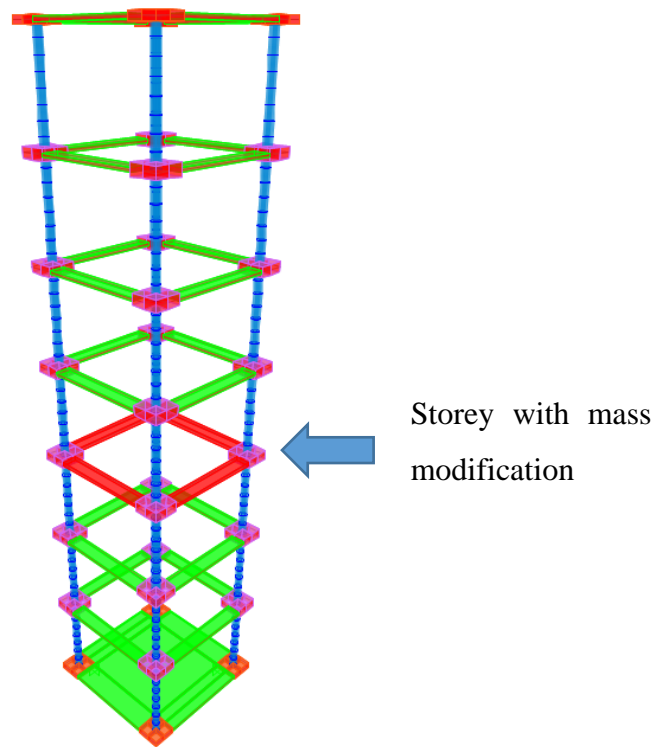

Figure B-1 Finite element model with the mass irregularity at 3rd storey

Mass is modified in the beam areas of the shell element with a mass modifier value of 8.41 based on the added mass on the experimental irregular model. This modification was done for each level per test and the resulting mode shape slope and mode shape curvature differences results were plotted to interpret the mass irregularity detection capability. The method with forward and backward difference method removed is used for this analysis. The graphs are given below.
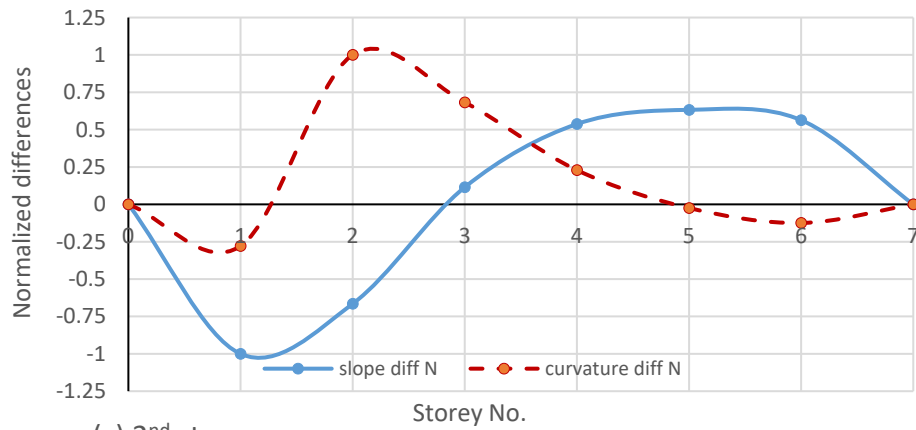
Figure B2- Difference in mode shape slopes (MSS) and mode shape curvatures (MSC) for **mass irregular model** with irregularity modelled at (a) base storey (b) 1st storey (c) 2nd storey (d) 3rd storey (e) 4th storey (f) 5th storey (g) 6th storey.
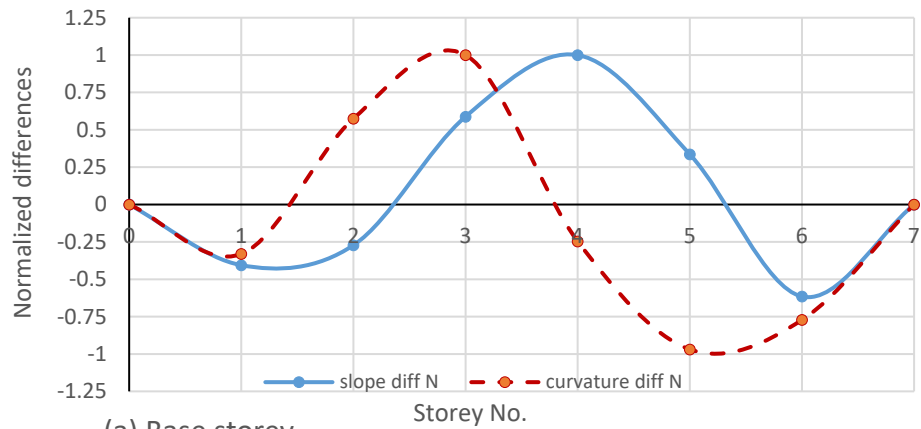
(a) Base storey
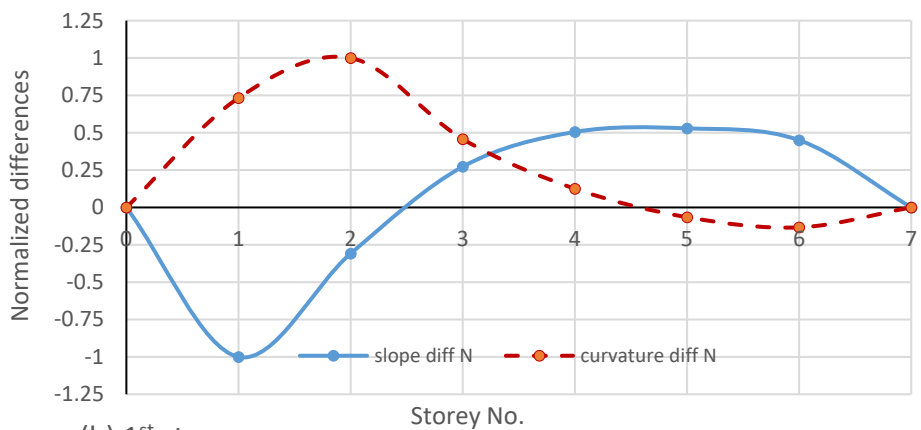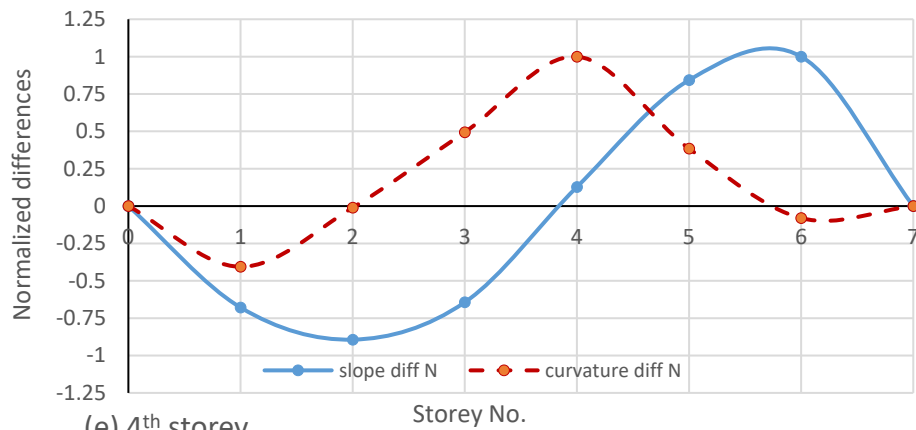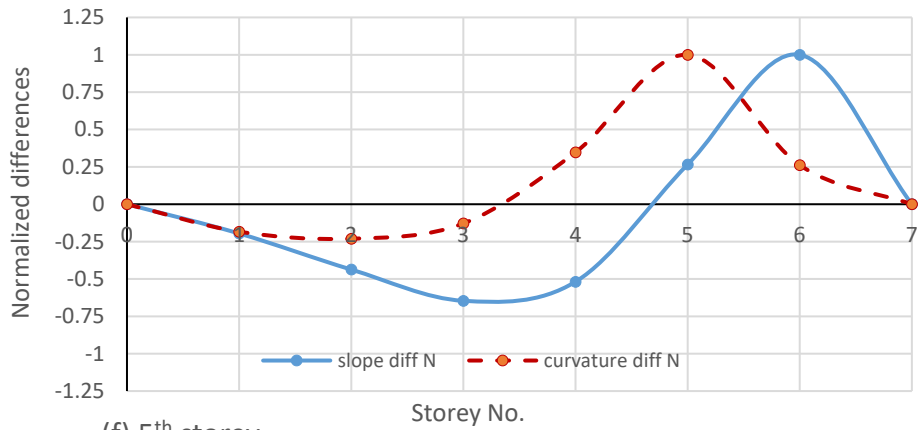

(b) 1st storey

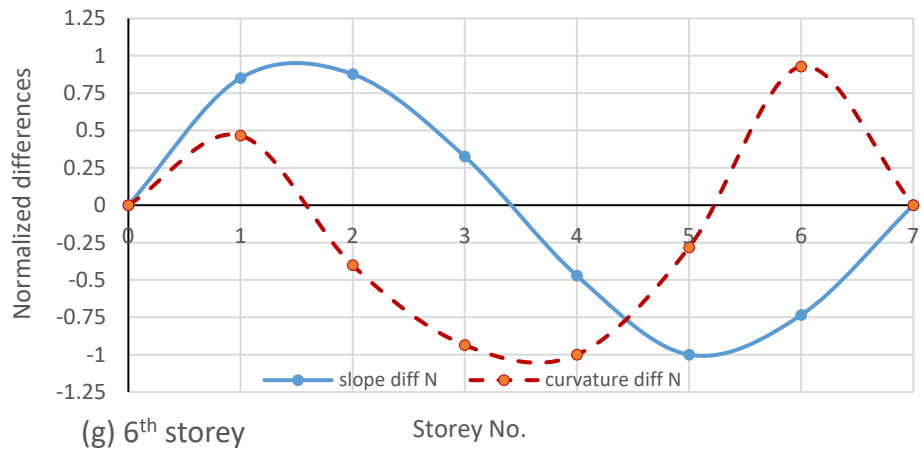(c) 2nd storey
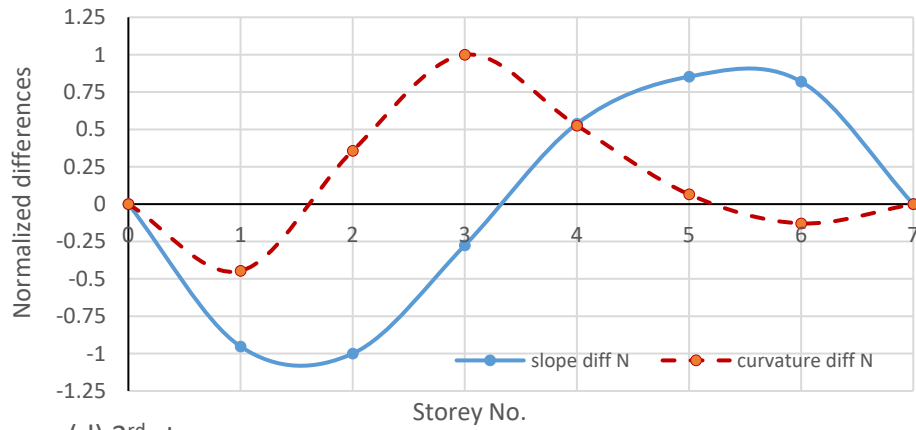
(d) 3rd storey

(e) 4th storey

(f) 5th storey

(g) 6th storey

Appendix C: Shaking Table and SINE SWEEP Module used in the study

Shaking table and accelerometer

The shaking table at the Department of Civil Engineering, University of Moratuwa belongs to the 1 degree of freedom ANCO R-201 shaking table family. The specifications are given in the Chapter 4.

The ANCO PC based closed loop program is provided with an equalizing controller with 4 input/output channels. The feedback from the accelerometer channels are used for equalization process to improve the fidelity of the table. The accelerometers used are piezoelectric DYTRAN 3055D2 series model with low noise, high sensitivity 50g and a 10-32 radial connector and stud mounting capabilities. This model enables general vibration testing and modal analysis and the base is isolated to avoid ground-loop interferences. The housing is titanium and is sealed to prevent errors in humid and dirty environments.

Figure C-1 DYTRAN3055D2 accelerometer used in the

shaking table (courtesy: www.dytran.com)

DANCE SINE SWEEP Module

The DANCE system consists of several modules, namely, Sweep Test Module, Spectime, Function generator, Transient Module, Chatter Module and IEEE344 Check Module. The SINE SWEEP Module is used in this study to apply a range of sine waves on the structure to determine the resonance frequency and amplitudes over the user defined range of frequencies. Apart from the sine waves, the module enables the application of sine beats sweeps and vibration aging tests. The software is capable of

adjusting its amplitudes based on the structure feedback to better fit the structure so that a faster process can be activated. The typical process of testing for one cycle can be listed as follows.
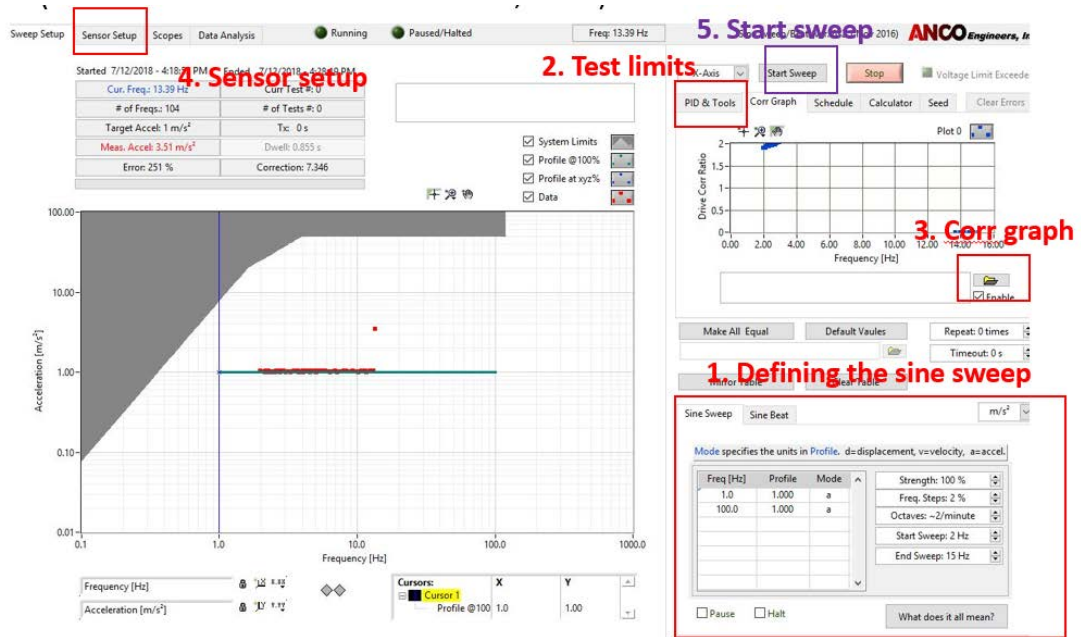

Figure C-2 Sine SWEEP module –steps of operation for one cycle

Defining the sine sweep and test limits, applying the correction graph, sensor setup (calibration values and defining location) and finally starting the sine sweep are the basic steps. The strength, frequency steps, start and end values of frequency are needed to define a sine sweep. Then the error upper and lower limits are chosen such that the iterations would be optimum and not excessive. After running the test the results are recorded and the DANCE software provides the acceleration-frequency response graph, transmissivity response graph, phase angle-frequency graph and tabulated responses of each sensor.

An acceleration-frequency graph for 4 sensors are given below. The natural frequency can be determined by observing the trend up to 6 decimal points and the respective frequency is used to calculate the velocity and amplitude values.
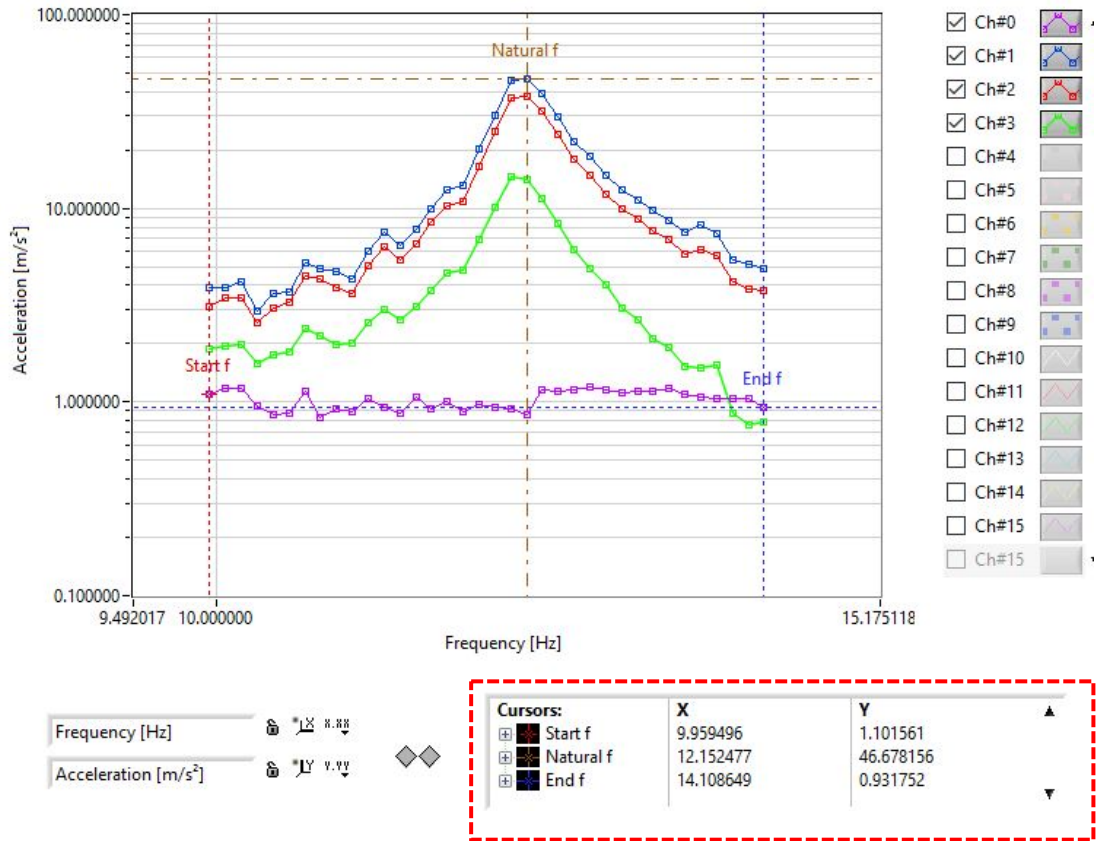
Figure C-3 Sample acceleration-frequency graph for 4 sensors